Edaravone Ameliorates Depressive and Anxiety-like Behaviors via Sirt1/Nrf2/HO-1/Gpx4 Pathway

Ruozhi Dang
The First Affiliated Hospital of Chongqing Medical University
Mingyang Wang
The First Affiliated Hospital of Chongqing Medical University
Xinhui Li
The First Affiliated Hospital of Chongqing Medical University
Haiyang Wang
The First Affiliated Hospital of Chongqing Medical University
Lanxiang Liu
The First Affiliated Hospital of Chongqing Medical University
Qingyuan Wu
Chongqing University Three Gorges Hospital
Jianting Zhao
Xinxiang Central Hospital
Ping Ji
Chongqing Medical University Stomatological Hospital
Lianmei Zhong
The First Affiliated Hospital of Kunming Medical University
Julio Licinio
SUNY Upstate Medical University College of Medicine
Peng Xie (xiepeng@cqmu.edu.cn)
The First Affiliated Hospital of Chongqing Medical University Department of Neurology
https://orcid.org/0000-0002-0081-6048

Research Article

Keywords: Edaravone, Depression, Anxiety, Oxidative stress, Gpx4, Ferroptosis

Posted Date: September 9th, 2021

DOI: https://doi.org/10.21203/rs.3.rs-850484/v1

Version of Record: A version of this preprint was published at Journal of Neuroinflammation on February 7th, 2022. See the published version at https://doi.org/10.1186/s12974-022-02400-6.

Abstract

Background: The inflammation and oxidative stress (OS) have been considered crucial components of the pathogenesis of depression. Edaravone (EDA), a free radical scavenger, processes strong biological activities including antioxidant, anti-inflammatory and neuroprotective properties. However, its role and potential molecular mechanisms in depression remain unclear. The present study aimed to investigate the antidepressant activity of EDA and its underlying mechanisms.

Methods: A chronic social defeat stress (CSDS) depression model was performed to explore whether EDA could produce antidepressant effects. C57BL/6J mice were intraperitoneally injected with EDA or Vehicle daily for 10 days. Behaviors tests were then carried out to examine depressive, anxiety-like and cognitive behaviors including social interaction (SI) test, sucrose preference test (SPT), open field test (OFT), elevated plus maze (EPM), novel object recognition (NOR), tail suspension test (TST) and forced swim test (FST). Hippocampal and medial prefrontal cortex (mPFC) tissues were collected for Nissl staining, immunofluorescence, targeted energy metabolomics analysis, measurement of MDA, SOD, GSH and transmission electron microscopy (TEM). Western blotting (WB) and quantitative real time polymerase chain reaction (qRT-PCR) detected the Sirt1/Nrf2/HO-1/Gpx4 signaling pathway. Knockdown experiments were performed to determine the effects of Gpx4 on CSDS mice with EDA treatment by an adeno-associated virus (AAV) vector containing miRNAi(GPX4)-EGFP infusion.

Results: The administrated of EDA dramatically ameliorated CSDS-induced depressive and anxiety-like behaviors. Additionally, EDA notably attenuated neuronal loss, microglial activation, astrocyte dysfunction, oxidative stress damage and energy metabolism in the hippocampus (Hip) and mPFC of CSDS-induced mice. Further examination indicated that the application of EDA after the CSDS model significantly increased the protein expressions of Sirt1, Nrf2, HO-1 and Gpx4 in the Hip. In addition, Gpx4 knockdown in CSDS mice abolished EDA-generated efficacy on depressive and anxiety-like behaviors.

Conclusion: These findings suggest that EDA possesses potent antidepressant and anxiolytic properties through Sirt1/Nrf2/HO-1/Gpx4 axis and Gpx4-mediated ferroptosis may play a key role in this effect.

Background

Major depression disorder (MDD), a common, debilitating psychiatric disorder, affects approximately 17 % of the population at some point in life [1, 2]. Although there are available antidepressants, most of the pharmacologic interventions take weeks to months to produce effects and have low response rates [3, 4]. Further, some striking studies have found that ketamine can produce rapid antidepressant effects, and its s-isomer, esketamine has been approved by the FDA to treat for adults with treatment-resistant depression [5, 6]. Although groundbreaking, some serious side effects, dissociative, psychotomimetic action and abuse potential limit its wide application. Therefore, novel therapies with fewer adverse effects and higher efficacy are urgently needed.

Accumulating evidence demonstrated a close link between oxidative stress (OS) and MDD [7, 8]. Generally, OS is defined as an imbalance between the oxidation and antioxidant capacity, involving reactive oxygen species (ROS) and reactive nitrogen species (RNS) [9]. ROS is involved in glutamate-dependent long-term potentiation (LTP) and moderate ROS is necessary for the growth and development of neurons [8]. Abundant studies showed that MDD was accompanied by decreased antioxidant and increased ROS status [8, 10, 11]. Moreover, preclinical and clinical evidence on OS and antioxidant effects of antidepressants addressed that they can scavenge ROS and RNS by scavenging free radicals and inhibiting OS pathways [11]. This process will protect neurons from the effect of OS and alleviate depression.

Silent information regulator 2 homolog 1 (Sirt1), a NAD^+ dependent protein deacetylase, regulates acetylation of specific transcription factors, proteins and is involved in abundant functions including energy metabolism, stress responses, inflammation and redox homeostasis [12, 13]. Specifically, recent studies have shown that Sirt1 plays a crucial role in depression and regulates downstream transcription factor including nuclear factor erythroid 2-related factor 2 (Nrf2) and NF-κB to prevent OS and inflammation damage [14–16]. Nrf2 is a primary transcription factor in the regulation of antioxidant response and has emerged as a potential therapeutic target for inflammatory disorders [17]. Dysregulation of Nrf2 leads to the decrease of antioxidants and detoxifying enzymes, which is involved in the pathogenesis of depression [18]. Heme oxygenase-1 (HO-1), a critical downstream target stress inducible protein of Nrf2, also exerts antioxidant stress and anti-inflammatory effects [19].

Ferroptosis, a recently discovered non-caspase-dependent form of programmed cell death, is characterized by the production of iron-dependent lipid ROS and associated with OS and inflammation [20, 21]. It differs from other types of cell death, such as apoptosis, autophagy, necrosis, and pyroptosis in morphological, physiological and genetically characteristics [22]. Both of Nrf2 and HO-1 could be inducible and participate in the synthesis of glutathione peroxidase 4 (Gpx4), which is the first discovered central inhibitor of ferroptosis [23]. Gpx4, a lipid repair enzyme, play a key role in the regulation of ferroptosis. Inhibition of Xc^- lead to depletion of cysteine and impaired the function of Gpx4, which eventually lead to ferroptosis [24]. Other studies have shown that Gpx4 can be upregulated by pro-inflammatory cytokines and overexpression of Gpx4 can prevent cell death from oxidative damage [25–27]. To the best of our knowledge, there is still no systematic research on the relation between ferroptosis and depression.

Edaravone (3-methyl-1-phenyl-2-pyrazolin-5-one, EDA), a free radical scavenger, processes strong biological activities including antioxidant, neuroprotective and anti-inflammatory effects [28]. It is commonly used to treat acute ischemic stroke and acute cerebral infarction. Moreover, EDA is effective in altering amyotrophic lateral sclerosis (ALS) progression, which is the second approved drug for treatment of ALS [29]. Recent studies have found that EDA exerts antioxidant and anti-inflammatory effects by Nrf2/HO-1 signaling pathway in asthma and cerebral infarction [30, 31]. Interestingly, only a few studies have addressed EDA can attenuated depressive-like behavior [32, 33]. However, the detailed molecular

mechanisms remain unclear. Accordingly, we hypothesized that EDA might ameliorate depressive and anxiety-like behaviors via Sirt1/Nrf2/HO-1/Gpx4 pathway.

To investigate this hypothesis, we established chronic stress defeated stress (CSDS) depression mice model and found EDA ameliorated depressive, anxiety-like behaviors and neuronal loss, affected energy metabolism, inhibited microglial activation and OS damage, attenuated astrocyte dysfunction and suppressed ferroptosis and inflammation response by regulating the Sirt1/Nrf2/HO-1/Gpx4 pathway. Furthermore, the pivotal role of Gpx4-mediated ferroptosis in EDA-related antidepressant and anxiolytic effects was confirmed using Gpx4 knockdown virus.

Materials And Methods

Animals and drugs treatment

Male C57BL/6J mice (aged 7–8 weeks) and retired male CD-1 mice (aged 16–20 weeks) were obtained from the Experimental Animal Centre of Chongqing Medical University (Chongqing, China). The experimental animals were housed in cages under a 12 h light/12 h dark cycle (lights on at 8:00 a.m.), 60 ± 5 % humidity, and a temperature of 23 ± 1 ℃ with access to water and food freely. All experimental procedures were conducted in accordance with the Ethics Committee of Chongqing Medical University. EDA was purchased from Sigma-Aldrich (St. Louis, USA) and was dissolved in Vehicle (NaCl, 0.9%) at a dosage of 10 mg/kg.

The study was conducted into two experiments.

In the first experiment, mice were randomly divided into three groups (10 each group): Control (CON) + Vehicle, CSDS + Vehicle and CSDS + EDA (10 mg/kg, intraperitoneally (i.p.)). The experiment schedule was shown in Fig. 1a. After 10 days CSDS model, mice were administered intraperitoneally (i.p.) daily injections of EDA or Vehicle for 10 days followed by behavioral tests and tissue collection.

To explore the Gpx4 role in CSDS-induced depression and anxiety, animals were randomized divided into six groups (10 each group), CON, CSDS, CSDS + Vehicle, CSDS + EDA, CSDS + EDA + CON-miRNAi and CSDS + EDA + Gpx4-miRNAi. The experiment schedule was shown in Fig. 10a.

Chronic social defeat stress (CSDS)

The CSDS paradigm was conducted as described previously [34]. Retired male CD-1 mice were screened for 3 consecutive days and the aggressors were selected according to the following criteria: (i) CD1 mice attacked the C57BL/6 J mice for 2 consecutive days and (ii) the latency to the initial attack on C57BL/6J mice was under 60 seconds (s). For 10 consecutive days, mice were placed in the home cage of CD1 and were defeated for 5 min. After physical defeat a perforated divider separated them for 24 hours (h) until the next physical defeat. Each day, intruder mice always faced a different resident. After 10 days of CSDS, retired male CD-1 mice and experimental mice were singly housed and performed 24 h later for the social interaction (SI) test.

SI test was composed of two stages. In the first stage, the experimental mice were allowed to explore an open field arena (44 cm × 44 cm × 30 cm) with an empty plastic box ((10 cm × 7 cm × 18cm)) for 2.5 min. In the second stage, a novel, aggressive CD-1 mouse was placed in the plastic box and was recorded for 2.5 min. The time of mice spent in the interaction zone (IZ) surrounding the plastic box was recorded and analyzed (Ethovision, Noldus, The Netherlands). For SI test, an SI ratio was calculated. SI ratio = time spent in interaction zone with a CD1 mouse / time spent in interaction zone without a CD1 mouse. Susceptible mice were defined by SI < 1, whereas resilient mice were defined by SI > 1. All mice used in the first experiment were susceptible mice.

Sucrose preference test (SPT)

Before the experiment, mice were habituated with two identical water bottles for 3 days. Each mouse was water and food-deprived for 24 h and then provided with 1 % water and sucrose solution. After 12 h, the bottles were weighted and the sucrose preference was calculated as (sucrose water intake/(sucrose water intake + pure water intake)) × 100 %.

Open field test (OFT)

A plain, 44 cm ×44 cm × 30 cm open field arena was used to assess the locomotor activity and anxiety-like behavior [35]. After a 30 s habituation, the total distance traveled, time spent in center arena (14.7 cm ×14.7 cm) was recorded in a 5 min session.

Elevated plus maze (EPM)

The EPM test was used to measure anxiety-related behavior in rodent [36]. The apparatus was composed of two closed arms (30 cm × 6 cm × 15 cm) and two open arms (30 cm×6 cm). Animals were placed in the EPM to explore for 5 min and time spent in closed and open arms was calculated.

Tail suspension test (TST)

Mice were suspended by the tails by using adhesive tape 1 cm from the tip of the tail and 15 cm above ground. Small plastic tubes were attached to tails to make sure mice could not climb. The tests lasted for 6 min and the immobility time was measured and analyzed during the final 4 min.

Forced swim test (FST)

Mice were placed individually into a transparent glass cylinder (diameter 15 cm, height 30 cm) filled with 15 cm depth of water (23 ± 1°C). The animals were placed in the cylinders for 6 min and the immobility time was calculated during the last 4 min.

Novel object recognition (NOR)

The NOR test was preformed according to previously protocols [37]. Briefly, the test was performed in an open field arena (44 cm ×44 cm × 30 cm). Objects were fixed to the open field arena and had different shapes, sizes and textures. The NOR test consists of two stages. During a 5 min acquisition phase, the animals were placed at the center of the arena in the presence of two identical objects (height: 12 cm;

base diameter: 7 cm). After 2 h, a 5 min retrieval phage was conducted and one of the two familiar objects was replaced by a novel object (6.5 cm ×6.5 cm × 6.5 cm). The time spent exploring familiar and novel objects was recorded and analyzed. The apparatus was cleaned with 75 % ethanol after each test. The “discrimination index” was calculated by the following [(novel object time)/ (novel object time + familiar object time)]. Object exploration was defined when the mice touch the object with its nose within 2 cm or less, and actively explore the objects.

Nissal staining

Nissl staining was preformed using Nissl staining solution (Beyotime, C0117, Shanghai, China) following the manufacturer’s protocols. The slides were observed under an optical microscope (Axio Image A2; Carl Zeiss, Germany) by a blinded investigator.

Immunofluorescence

The brain sections (20 um thick) were washed in PBS for 5 min three times, blocked with 5 % bovine serum albumin (BSA) and 0.2 % Triton X-100 for 2 h at room temperature. After blocking, the sections were incubated with primary antibodies overnight at 4°C, and then sequentially incubated with the secondary antibodies for 2 h at room temperature. Primary antibodies include: Rabbit anti-Iba-1 (1:500, Wako, 019-19741), Goat anti-GFAP (1:500, Abcam, ab53554). The nuclei were counterstained with DAPI for 10 min. Fluorescent images were captured with a fluorescence microscope (VS200; Olympus, Japan) and confocal microscope (A1R, Nikon, Japan).

Transmission electron microscopy (TEM)

Mice were anesthetized and perfused with phosphate-buffered solution (PBS) followed by 4 % paraformaldehyde. Small hippocampus (Hip) and medial prefrontal cortex (mPFC) tissues (1 mm^3) were quickly dissected and post-fixed overnight at 4°C using 2.5 % glutaraldehyde. Tissues were embedded and cut into along the coronal plane at a thickness of 60–80 nm. The mitochondrial morphology was detected by transmission electron microscope (JEM-1400 PLUS, Japan) by a blinded pathologists.

Measurement of MDA, SOD and GSH

The activities of the antioxidant enzymes of MDA, SOD and GSH within Hip and mPFC tissues were measured with the malondialdehyde (MDA) activity assay kit (No.A003-1-2), the superoxide dismutase (SOD) activity assay kit (No.A001-3-2) and GSH activity assay kit (No.A006-2-1). All measurements were performed using tissue homogenate with standard protocols. All kits were purchased from Jiancheng Inc. (Nanjing, China).

LC-MS/MS analysis

LC-MS/MS was conducted according to previous studies [38]. Briefly, 30 mg brain tissues were preconditioned with 200 μl cool ultrapure water for homogenization. Then 800 μl methanol/acetonitrile (1:1, v/v) were added and the mixture was sonicated twice for 30 min and placed 1 h at -20 ℃ to precipitate proteins. After centrifugation, the supernatants were dried and collected. The analysis of

supernatants was conducted with Agilent 1290 Infinity LC chromatography system and AB SCIEX 5500 QTRAP mass spectrometer.

Western blotting (WB)

The Hip and mPFC tissues were dissociated by radio-immunoprecipitation assay solution containing protease inhibitors and phosphatase inhibitor. The proteins in the samples were run on 10 % SDS polyacrylamide gel and then transferred to polyvinylidene fluoride membrane (Millipore, USA). The proteins were incubated with Rabbit anti-Sirt1(abcam, #ab189494;1:1000), Rabbit anti-Nrf2 (proteintech, #16396-1-AP;1:1000), Rabbit anti-HO-1 (proteintech, #10701-1-AP;1:1000), Rabbit anti-Gpx4 (abcam, #ab125066;1:3000), mouse anti-GAPDH (abcam, #ab8245;1:10000), mouse anti-Chop (Cell Signaling ,#2895,1:1000) overnight at 4°C, and secondary anti-mouse HRP-conjugated (Bio-rad, cat# 170–6516,1:10000) or secondary anti-rabbit HRP-conjugated antibodies (Bio-rad, # 170–6515,1:10000) were incubated for 2 h at room temperature. The signals were visualized using ECL chemiluminescence reagent (Beyotime; US Everbright Inc.).

Quantitative real-time polymerase chain reaction (qRT-PCR)

Total RNA in Hip and mPFC lysates of mice were extracted with TRIzol reagent (Invitrogen, Carlsbad, CA) and reverse transcribed into cDNA by PrimeScript RT reagent Kit (Takara, Japan) following the manufacturer's guides. Relative mRNA expression levels were performed with SYBR Green detection system (Roche, Germany). All samples were performed in triplicate and normalized with β-actin mRNA level. The primer sequences are listed in Table 1.

Table 1
Primer sequences used in the qRT-PCR

Gene	Primer sequences
Sirt1	Forward:5'-GCTGACGACTTCGACGACG-3'
	Reverse:5'-TCGGTCAACAGGAGGTTGTCT-3'
Nrf2	Forward:5'-TCTTGGAGTAAGTCGAGAAGTGT-3'
	Reverse:5'-GTTGAAACTGAGCGAAAAAGGC-3'
HO-1	Forward:5'-AAGCCGAGAATGCTGAGTTCA-3'
	Reverse:5'-GCCGTGTAGATATGGTACAAGGA-3'
Gpx4	Forward:5'-CTGCTCTTCCAGAGGTCCTG-3'
	Reverse:5'-GAGGTGTCCACCAGAGAAGC-3'
NF-κB	Forward:5'-ATGGCAGACGATGATCCCTAC-3'
	Reverse:5'-TGTTGACAGTGGTATTTCTGGTG-3'
cGAS	Forward:5'-GAGGCGCGGAAAGTCGTAA-3'
	Reverse:5'-TTGTCCGGTTCCTTCCTGGA-3'
STING	Forward:5'-GGTCACCGCTCCAAATATGTAG-3'
	Reverse:5'-CAGTAGTCCAAGTTCGTGCGA-3'
TBK1	Forward:5'-ACTGGTGATCTCTATGCTGTCA-3'
	Reverse:5'-TTCTGGAAGTCCATACGCATTG-3'
β-actin	Forward:5'-ACTGCCGCATCCTCTTCCT-3'
	Reverse:5'-TCAACGTCACACTTCATGATGGA-3'

Stereotaxic virus injection

Mice were anesthetized with isoflurane and then placed on a stereotaxic apparatus (RWD, Shenzhen, China). Virus was injected using Nanoject II (Drummond Scientific, PA) via a micro pipette. 3 min after pipette insertion, small amounts of virus were multiple injected at 30 s intervals (13 nl/s). After waiting for 10 min, the pipette was slowly retracted. 2 μl AAV2/8-CMV-EGFP-miRNAi(Gpx4) or AAV2/8-CMV-EGFP-miRNAi(NC) (Taitool, Shanghai, China) was bilaterally injected into the Hip (coordinates, bregma: AP = -1.70 mm; ML = ± 1.25 mm; DV = -1.20 mm, bregma: AP = -3.15 mm; ML = ± 2.94 mm; DV = -3.62, -2.25 mm,). Behavioral tests were commenced 4 weeks after viral injection.

Statistical analysis

Data were presented as mean ± SEM and analyzed with GraphPad Prism 8.0 or the statistical program SPSS 17.0. The normality of data was assessed individually and non-parametric test were used when $p < 0.05$. Homogeneity of variance was be verified by Brown-Forsythe test, when $p < 0.05$, data were analyzed by one way analysis of variance (ANOVA) followed by Dunnett's T3 post hoc test. Statistical comparisons among groups were performed by using ANOVA followed by Tukey's test or Fisher's LSD (data for energy metabolites in Fig. 7) post hoc test for normal distributed data and Kruskal-Wallis test with multiple comparisons for non-normal distributed data. $p < 0.05$ was regarded as significant.

Results

EDA ameliorates depression and anxiety-related behaviors after CSDS exposure

To investigate the effect of EDA on depression, we exposed mice to a well-established animal model of depression, CSDS, and subsequently preformed multiple behavioral tests including SI, SPT, OFT, NOR, EPM, TST, and FST (Fig. 1a). As shown in Fig. 1b-c, mice exposed to CSDS showed significantly decreased SI ratio. However, intraperitoneal injection of EDA improved the SI ratio as compared to the CSDS + Vehicle group. In SPT, the consumption of sucrose was significantly reduced in CSDS exposed mice compared with the control mice. Nevertheless, EDA intervention greatly reversed CSDS-induced reduction in sucrose preference, which reflected anhedonia (Fig. 1d). Next, mice, exposed to an inescapable aversive environment TST and FST, initially violent escape but then transition to a passive coping (PC) state [39]. This state can be intervened by pharmacological approach and may be associated with the pathological motivational impairments in MDD [40, 41]. We found that CSDS + Vehicle animals exhibited a robust increase immobility in TST and FST. As expected, CSDS + EDA mice exhibited significant decreases in time spent immobile compared to CSDS + Vehicle mice (Fig. 1f-g). These results consistently indicate that EDA elicits antidepressant effect in mice.

In addition, we employed OFT and EPM to evaluate anxiety-like behavior. The CSDS + Vehicle mice exhibited remarkable anxiety-like behavior relative to the controls, as indicated by less time spent in center zone of OFT and the open arms in the EPM. Nevertheless, this reduction was markedly reversed by the administration of EDA, indicating EDA was effective in ameliorating CSDS-evoked anxiety (Fig. 1e, j).

Previous study has observed oral administration of EDA ameliorated the AD-like pathologies and memory deficits of the mice [42]. Accordingly, we carried out the NOR test to determine whether EDA affects the recognition memory of mice (Fig. 1h-i). Interestingly, there was no difference in time spent with the novel object among all groups, displayed no impairment of object memory retention.

EDA treatment significantly alleviates neuronal injury

MDD was thought to be primarily triggered through neuronal dysfunction in the Hip and mPFC [43]. Based on existing evidence, Nissl staining was employed to observe neuronal morphological changes in the Hip and mPFC. As showed in Fig. 2a, c, neurons in the hippocampal CA1 and mPFC regions were

arrayed regularly and compactly and Nissl bodies were clear in the CON + Vehicle group. Whereas, CSDS-evoked mice have increased damaged neurons, which were irregular and sparsely distributed as well as Nissl body disintegrated compared with the CON + Vehicle group. The number of Nissl-positive cells was observably reduced compared with the CON + Vehicle group. After EDA administration, the decrease of Nissl-positive neurons and neuronal damage were ameliorated (Fig. 2b, d). These data indicated that EDA could attenuate CSDS-induced neuronal damage.

EDA inhibits microglial activation and attenuates astrocyte dysfunction in the CSDS exposed mice

Neuroinflammation is tightly associated with the onset of depression [44, 45]. Given that microglia and astrocytes play an essential role in neuroinflammation and undergo abnormally structural and functional changes in Hip and mPFC in response to chronic stress, we first examined the effect of EDA on the distribution and morphology of microglia in the Hip and mPFC using ionized calcium-binding adaptor molecule 1 (Iba-1) staining (Fig. 3a, e). The hippocampal and mPFC microglia exhibited striking activation morphology after CSDS exposure, as indicated by increased cell number, total branch length and branch number. These effects were significantly alleviated by EDA administration (Fig. 3b-d, f-h).

Since CSDS mice experience neuroinflammation leading to astrocyte dysfunction, we then examined the effect of EDA on astrocyte morphology and characteristics. This finding was confirmed by glial fibrillary acidic protein (GFAP) staining (Fig. 4a, e). CSDS exposure resulted in astrocyte dysfunction in CSDS + Vehicle mice, as indicated by the fact that CSDS exposure decreased the number of GFAP-positive cells and by the ramification of astrocytes characterized by the significantly decreased branch numbers and length. As expected, administration of EDA remarkably alleviated astrocyte dysfunction (Fig. 4b-d, f-h).

Together, these results suggest that EDA ameliorates CSDS-induced depressive and anxiety-like behaviors through inhibiting microglial activation and alleviating astrocyte dysfunction.

Effects of EDA on OS and mitochondrial damage in the Hip and mPFC

Given OS is emerging as an important therapeutic target for MDD, we measured the activities of MDA, SOD and GSH in the Hip and mPFC to evaluate the effect of EDA on OS induced lipid peroxidation. As shown in Fig. 5a-b, the activities of SOD and MDA were significantly decreased in the Hip of CSDS + Vehicle mice. In contrast, the content of GSH in the CSDS + Vehicle group was notably higher than the CON + Vehicle group. However, intraperitoneal injection of EDA completely reversed these alterations (Fig. 5a-c). In the mPFC tissue, CSDS exposure significantly decreased MDA level. After EDA application, mice in the CSDS + EDA group recovered MDA and GSH activities (Fig. 5e, f). Nevertheless, SOD activity had no changes among three groups (Fig. 5d).

Since the antioxidant property of EDA was mitochondria-mediated, we used TEM to observe mitochondrial damages in the Hip and mPFC. CSDS exposure exhibited profound effects on

mitochondrial structure, including mitochondrial swelling and loss of mitochondrial cristae in neuron (Fig. 6) and microglia (Fig. S1). In addition, compared with the CSDS + Vehicle group, EDA treatment alleviated these pathological changes. Interestingly, Hip mitochondrial damage was more severe than in the mPFC region (Fig. 6a-b; Fig. S1a-b). Altogether, these findings implied that EDA might ameliorated CSDS-induced OS and mitochondrial damage.

EDA treatment affects energy metabolites in the Hip and mPFC

Given EDA was a potent mitochondrial antioxidant and metabolism enhancer, we carried out targeted energy metabolomics analysis with detecting 32 metabolites in the Hip and mPFC tissues of mice. The heat maps of metabolites changes of CON + Vehicle vs. CSDS + Vehicle vs. CSDS + EDA were shown in Fig. 7a-b. In the Hip, the GMP, NADP, GDP and AMP in the CSDS + Vehicle group were reduced related to the CON + Vehicle group without statistical significance. However, these metabolites were significantly increased in the CSDS + EDA group compared with CSDS + Vehicle group (Fig .7c-f). In addition, Beta-D-Fructose 6-phosphate in the CSDS + Vehicle group was notably diminished compared with CON + Vehicle group (Fig .7g). In the mPFC, we found most of the energy related metabolites were not changed by CSDS exposure. Nevertheless, Succinate and ADP were significantly decreased in CSDS + Vehicle group compared with CON + Vehicle group (Fig .7h, i). Meanwhile, compared with CSDS + Vehicle group, 4 metabolites (GMP, ADP, AMP and GDP) were markedly increased in the CSDS + EDA group (Fig. 7i-l). Among the differentially altered metabolites, GMP, GDP and AMP were altered in both the Hip and mPFC tissues, with the other metabolites altered either in Hip or mPFC.

Then, we used Ingenuity Pathway Analysis (IPA) to identify the top canonical signaling pathways affected in Hip and mPFC with or without EDA treatment. Each of the top 5 canonical pathways were exhibited in Fig. S2. Of all these pathways, we noticed that NAD salvage pathway in the Hip was associated with the antioxidant mechanism of EDA. The NAD salvage pathway was the main source of NAD^+ biosynthesis in mammalian cells [46]. Interestingly, Sirt1 is an NAD^+ dependent histone deacetylase and medicates levels of anxiety and depression [47].

Furthermore, we used Kyoto Encyclopedia of Genes and Genomes (KEGG) database to reveal the function of differential metabolites in signaling pathways. Remarkably, the significant alternation of NADP in the Hip might indicated a potential relevance between glutathione metabolism and depression.

Taken together, these results demonstrated that EDA administration significantly affected energy metabolites in the Hip and mPFC. Further, changes in hippocampal energy metabolites might be more associated with depression in contrast with mPFC.

EDA reverses CSDS-induced depression and anxiety via Sirt1/Nrf2/HO-1/Gpx4 pathway

Given Gpx4 and Nrf2 plays a crucial role in glutathione metabolism and Sirt1's involvement in MDD, we next sought to examine the role of Sirt1/Nrf2/HO-1/Gpx4 pathway in EDA-related depression and anxiety by WB. As shown in Fig. 8a-f, CSDS exposure robustly decreased the expression levels of Sirt1, Nrf2, HO-1 and Gpx4 and increased the expression levels of Chop in the Hip. However, these effects were significantly reversed by the treatment with EDA. In the mPFC, the protein expression level of Sirt1 was significantly higher in CSDS + EDA group as compared to the CSDS + Vehicle group, and the expression level of Chop was notably lower in CSDS + EDA group as compared to the CSDS + Vehicle group (Fig. 8h, l). Nevertheless, the CSDS + Vehicle and CSDS + EDA groups had no significant effects on the levels of Nrf2, HO-1 and Gpx4 (Fig. 8i, j, k).

We further examine the mRNA levels of Sirt1/Nrf2/HO-1/Gpx4 and cGAS/STING/TBK1 pathways in the Hip and mPFC. As exhibited in Fig. 9, CSDS + Vehicle group was found with significantly upregulated mRNA (Nrf2, HO-1 and NF-κB) in the Hip and mPFC as compared to CON + Vehicle group. Rather, within exposure to EDA, we found decreased expressions of NF-κB, Nrf2 and HO-1 in both Hip and mPFC compared with CSDS + Vehicle group. Also, we detected that Sirt1 and TBK1 mRNA levels were dramatically enhanced in CSDS + Vehicle group compared to CON + Vehicle group of mPFC tissue, but not in Hip tissue (Fig. 9h, n). As expected, Sirt1 and TBK1 mRNA levels were reduced in CSDS + EDA group compared to CSDS + Vehicle group of mPFC. Further, we observed no difference in mRNA levels of cGAS, STING, TBK1 and Gpx4. These results suggest that EDA can rescue the depression and anxiety-like behaviors via Sirt1/Nrf2/HO-1/Gpx4 pathway.

Blockade of Gpx4 abolishes the antidepressant and anxiolytic effects of EDA

Previous studies have confirmed that Sirt1 and Nrf2 played an important role in depression [18, 48]. It remains unknown, however, whether Gpx4-regulated ferroptosis affect the antidepressant and anxiolytic effects of EDA. Accordingly, an adeno-associated virus (AAV) vector that selectively expresses Gpx4-miRNAi with enhanced green fluorescent protein (AAV-EGFP-Gpx4-miRNAi) was injected into the Hip of mice. Then CSDS depression model was performed, followed by behavior tests by SI, SPT, OFT, NOR, EPM, TST, and FST (Fig. 10a). As shown in Fig. 10b-e, mice exposed to EDA showed markedly increased SI ratio in SI, sucrose consumption in SPT, center time in OFT and open arms time in EPM as compared to the CSDS group, whereas compared to the CSDS + EDA group, the AAV-EGFP-Gpx4-miRNAi treatment decreased SI ratio, center time and open arms time, but not sucrose consumption. As shown in Fig. 10f-g, immobility time in TST and FST were significantly decreased in the CSDS + EDA group as compared to the CSDS group. However, compared to the CSDS + EDA group, immobility time in TST and FST in the CSDS + EDA + Gpx4-miRNAi group were dramatically increased. Intriguingly, the discrimination index exhibited markedly decreased in the CSDS + EDA + Gpx4-miRNAi group as compared to the CSDS + EDA group (Fig. 10h). These data indicated that the antidepressant and anxiolytic effects of EDA in CSDS-induced mice was blocked by AAV-EGFP-Gpx4-miRNAi.

Discussion

In the present study, we demonstrated that the antidepressant and anxiolytic properties of EDA and its potential mechanism (Fig. 11). Current studies indicated that EDA attenuated CSDS-evoked depressive symptoms and CSDS-induced anxiety behaviors, and the underlying mechanisms were associated with the alteration of expression of Sirt1/Nrf2/HO-1/Gpx4 pathway in the Hip. The knockdown of Gpx4 in the Hip abolished the effects of EDA treatment. Furthermore, EDA protected microglia and astrocyte against CSDS-induced inflammation alternations, attenuated neuronal damage in the Hip and mPFC. These results shed light on the antidepressant and anxiolytic effects of EDA and provide a new idea about the Gpx4-regulated ferroptosis in depression and anxiety.

To the best of our knowledge, this study is the first to demonstrate that the antidepressant and anxiolytic effects of EDA was brain region-specific. EDA is a free radical scavenger that can pass through the blood brain barrier (BBB) and has therapeutic effects on stroke and ALS [29, 49]. Only a few studies indicated that high concentrations of EDA presents antidepressant-like activity in chronic restraint stress and corticosterone model of depression [32, 33]. Here, we first evaluated the effect of EDA on CSDS-induced depressive behaviors. As expected, administration of EDA ameliorated depressive and anxiety like behaviors.

Recent study confirms that MDD is associated with hippocampal and mPFC structural aberrations, including cellular damage, volumetric reductions and reduced hippocampal neurogenesis [50, 51]. Thus, we focus on both Hip and mPFC and sought to explore whether the antidepressant and anxiolytic effects of EDA are present in specific region of the brain. Here, we found that the anti-neuroinflammatory effect of EDA in CSDS-induced depressed mice was associated with inhibiting the increase of microglial activation and mitigating astrocyte dysfunction in the Hip and mPFC regions. In addition, the neuronal death in the Hip and mPFC was relieved with treatment of EDA.

OS is the imbalance between the production of ROS and antioxidant capacity and plays a pivotal role in MDD. Increased ROS and molecules controlled by OS are related to the pathogenesis and progression of MDD [9, 10]. Furthermore, OS and inflammation are interdependent and functionally complementary, which are ubiquitous in MDD. Mounting evidence indicated that inflammation may affect mitochondrial function, membrane polarity and oxidative phosphorylation, which may further lead to oxidative stress and apoptosis [11, 52–54]. Microglia and astrocytes are main mediators of inflammation in the brain [55]. In our study reported here, the EDA administration significantly decreased microglial activation and attenuated astrocyte dysfunction. In addition, our research indicated that EDA alleviated OS damage and the Hip was the main site of this effect.

Increasing evidence indicated that mitochondrial dysfunctions have been deemed as the underlying mechanism of MDD and the increase of ROS is associated with the reduction in neuronal metabolism [56, 57]. This metabolic deterioration is associated with reduced activity of ATP synthesis, primarily due to mitochondrial dysfunction. According to the “mitochondrial bioenergetics hypothesis”, depression is the most common psychiatric disorder in patients with impaired mitochondrial functions [57]. Given the most prominent role of mitochondria is the production of energy, we then preformed TEM and targeted

energy metabolomics to further explore the mitochondrial dysfunctions and abnormal energy metabolism in the Hip and mPFC tissues of depression. Previous works have shown significant disturbances of energy metabolism in CSDS, chronic unpredictable mild stress (CUMS), learned helplessness, and chronic restraint stress model of mice [38, 58]. In our study, intraperitoneal injection of EDA greatly improved the mitochondrial and energy metabolism dysfunctions. Of note, mitochondrial damage in the Hip was more severe than in the mPFC region.

The changes of energy metabolism pathway are involved in the Krebs cycle and glycolysis. We then used IPA and KEGG to analyze the differentially metabolites. It is worth noting that NAD salvage pathway through IPA and glutathione metabolism via KEGG pathway enrichment in the Hip might be associated with the antioxidant mechanism of EDA. Sirt1, a NAD^+-dependent deacetylase, plays a key role in NAD salvage pathway and medicates levels of anxiety and depression [47, 48]. Sirt1 expression was markedly reduced in the blood of MDD patients compared with healthy subjects [59]. Moreover, the Sirt1 activity in dentate gyrus of Hip was decreased when chronic stress exposure and genetic or pharmacologic ablation of Hip Sirt1 can lead to depression [60]. Nrf2, an important antioxidant, is an important downstream target of Sirt1 and plays a crucial role in improving the resistance to oxidative stress damage. Previous studies showed that Nrf2 knockout mice exhibited depressive-like behavior and CUMS model decreased Nrf2 expression in the rat Hip [61, 62]. Besides, corticosterone treated mice showed lower level of Nrf2 protein expression in the cortex and Hip [63]. Recently, accumulating evidence revealed that a close link between Nrf2/HO-1 pathway and MDD [63, 64]. It is mentioned above that we found the difference in glutathione metabolism via KEGG pathway enrichment. Interestingly, the gene of Gpx4 plays a key role in glutathione metabolism and Nrf2 can directly or indirectly regulate Gpx4 protein expression and function [65].

Therefore, we speculated that EDA improved depressive and anxiety-like behaviors by activating the Sirt1/Nrf2/HO-1/Gpx4 signaling pathway. Here, we observed that mice underwent CSDS exposure displayed reduced protein expressions of Sirt1, Nrf2, HO-1 and Gpx4 in the Hip and Sirt1 in the mPFC, which were all elevated by EDA intervention. The reasons for the divergent results between the Hip and mPFC are unclear, but one possibility may due to different brain structure and cellular component. Interestingly, mRNA levels of Nrf2, HO-1 in the Hip and Sirt1, Nrf2, HO-1 in the mPFC increased after CSDS exposure, whereas reversed by EDA treatment. We deduced that the opposite results between mRNA and protein levels may owe to the regulation of transcriptional or post-translational protein modification.

Nrf2 and Gpx4 are important regulators of STING and neuroinflammation, an innate immune response to tissue damage, plays a vital role in MDD [66–68]. Thus, we explored the innate immune cGAS/STING/TBK1 pathway in mRNA level. Disappointedly, only TBK1 mRNA in the mPFC has been changed.

Ferroptosis is a recent identified type of regulated cell death and has also been reported to be associated with several neurological diseases, including neurodegeneration, stoke and neurotrauma [69]. However, there is still lack of report about ferroptosis in the psychiatric diseases, especially depression and anxiety.

Gpx4 was identified as a key regulatory factor in ferroptosis and the protein expression of Gpx4 changed after CSDS exposure in the Hip, but not in the mPFC. Hence, we then knockdown of Gpx4 in the Hip to explore the role of Gpx4-related ferroptosis in the effects of EDA. Strikingly, EDA-induced antidepressant and anxiolytic effects was abolished. Unexpectedly, the object recognition memory was impaired after AAV-eGFP-Gpx4-miRNAi injection, indicating that Gpx4 may be associated with memory impairment.

Nevertheless, our study is not without limitations. First, the pathway from Sirt1 to Gpx4 is complex and we targeted only one portion of this pathway. Second, EDA alleviated neuroinflammtion and neuronal loss in both the Hip and mPFC. Hence, we could not rule out the possibility that other mechanisms in the mPFC may underlie the functions of EDA. Third, although we demonstrated Gpx4 plays a key role in the effects of EDA, further research is required to investigate the Gpx4-related ferroptosis in depression and anxiety.

Conclusion

In summary, our study demonstrates for the first time that EDA could ameliorate depressive and anxiety like behavior, oxidative stress and neuroinflammation in a CSDS-induced mice model of depression. The underlying molecular mechanism may involve Gpx4-mediated ferroptosis via Sirt1/Nrf2/Ho-1 pathway.

These results also highlight aberrant expression of Gpx4 as a potential mechanism in depression and suggest that Gpx4 mediated ferroptosis may be a promising new target for the treatment of MDD.

Abbreviations

OS: Oxidative stress; EDA: Edaravone; CSDS: Chronic social defeat stress; MDD: Major depression disorder; SI: Social interaction; SPT: Sucrose preference test; OFT: Open field test; EPM: Elevated plus maze; NOR: Novel object recognition; TST: Tail suspension test; FST: Forced swim test; TEM: Transmission electron microscopy; WB: Western blotting; qRT-PCR: Quantitative real time polymerase chain reaction; AAV: Adeno-associated virus; Hip: Hippocampus; mPFC: Medial prefrontal cortex; RNS: Reactive nitrogen species; LTP: Long-term potentiation; Sirt1: Silent information regulator 2 homolog 1; Nrf2: Nuclear factor erythroid 2-related factor 2; HO-1: Heme oxygenase-1; Gpx4: Glutathione peroxidase 4; FDA: Food and Drug Administration; ALS: Amyotrophic lateral sclerosis; CON: Control; IZ: Interaction zone; MDA: Malondialdehyde; SOD: Superoxide dismutase; GSH: Glutathione; ANOVA: Analysis of variance; IPA: Ingenuity Pathway Analysis; AMP: Adenosine monophosphate; GMP: Guanosine monophosphate; GDP: Guanosine diphosphate; ADP: Adenosine diphosphate; KEGG: Kyoto Encyclopedia of Genes and Genomes; cGAS: Cyclic GMP-AMP synthase; STING: Stimulator of interferon genes; TBK1: TANK binding kinase; GAPDH: Glyceraldehyde 3-phosphate dehydrogenase; CUMS: Chronic unpredictable mild stress; BBB: Blood brain barrier; GFAP: Glial fibrillary acidic protein; Iba-1: Ionized calcium-binding adaptor molecule 1; PBS: Phosphate-buffered solution; PC: Passive coping; AD: Alzheimer's disease; CHOP: C/EBP homologous protein.

Declarations

Acknowledgements

Not applicable.

Authors' contributions

PX and RZD designed the experiments; RZD, MYW and XHL performed the experiments; HYW, LXL, QYW, and JTZ assisted with experiments; RZD and XHL analyzed the data; RZD wrote the manuscript; PJ, LMZ, JL and PX revised the manuscript. The authors read and approved the final manuscript.

Funding

This work was supported by the National Key Research and Development Program of China (Grant No. 2017YFA0505700), the Non-Profit Central Research Institute Fund of Chinese Academy of Medical Sciences (Grant No. 2019PT320002), and the Natural Science Foundation Project of China (Grant No. 81820108015).

Availability of data and materials

All data generated in this study are included in this manuscript.

Ethics approval and consent to participate

All experimental procedures were conducted in accordance with the Ethics Committee of Chongqing Medical University.

Consent for publication

Not applicable.

Competing interests

The authors declare no conflict of interest.

References

1. Belmaker RH, Agam G. Major depressive disorder. N Engl J Med. 2008;358(1):55–68. https://doi.org/10.1056/NEJMra073096.
2. Hasin DS, Sarvet AL, Meyers JL, Saha TD, Ruan WJ, Stohl M, et al. Epidemiology of adult DSM-5 major depressive disorder and its specifiers in the United States. JAMA Psychiatry. 2018;75(4):336–46. https://doi.org/10.1001/jamapsychiatry.2017.4602.

3. Mrazek DA, Hornberger JC, Altar CA, Degtiar I. A review of the clinical, economic, and societal burden of treatment-resistant depression: 1996-2013. Psychiatr Serv. 2014;65(8):977–87. https://doi.org/10.1176/appi.ps.201300059.
4. Murrough JW, Abdallah CG, Mathew SJ. Targeting glutamate signalling in depression: progress and prospects. Nat Rev Drug Discov. 2017;16(7):472–86. https://doi.org/10.1038/nrd.2017.16.
5. Kim J, Farchione T, Potter A, Chen Q, Temple R. Esketamine for treatment-resistant depression - first FDA-approved antidepressant in a new class. N Engl J Med. 2019;381(1):1–4. https://doi.org/10.1056/NEJMp1903305.
6. Li N, Lee B, Liu RJ, Banasr M, Dwyer JM, Iwata M, et al. mTOR-dependent synapse formation underlies the rapid antidepressant effects of NMDA antagonists. Science. 2010;329(5994):959–64. https://doi.org/10.1126/science.1190287.
7. Black CN, Bot M, Scheffer PG, Cuijpers P, Penninx BW. Is depression associated with increased oxidative stress? A systematic review and meta-analysis. Psychoneuroendocrinology. 2015;51:164–75. https://doi.org/10.1016/j.psyneuen.2014.09.025.
8. Bhatt S, Nagappa AN, Patil CR. Role of oxidative stress in depression. Drug Discov Today. 2020;25(7):1270–6. https://doi.org/10.1016/j.drudis.2020.05.001.
9. Maes M, Galecki P, Chang YS, Berk M. A review on the oxidative and nitrosative stress (O&NS) pathways in major depression and their possible contribution to the (neuro)degenerative processes in that illness. Prog Neuropsychopharmacol Biol Psychiatry. 2011;35(3):676–92. https://doi.org/10.1016/j.pnpbp.2010.05.004.
10. Lindqvist D, Dhabhar FS, James SJ, Hough CM, Jain FA, Bersani FS, et al. Oxidative stress, inflammation and treatment response in major depression. Psychoneuroendocrinology. 2017;76:197–205. https://doi.org/10.1016/j.psyneuen.2016.11.031.
11. Xu Y, Wang C, Klabnik JJ, O'Donnell JM. Novel therapeutic targets in depression and anxiety: antioxidants as a candidate treatment. Curr Neuropharmacol. 2014;12(2):108–19. https://doi.org/10.2174/1570159X11666131120231448.
12. Sauve AA, Wolberger C, Schramm VL, Boeke JD. The biochemistry of sirtuins. Annu Rev Biochem. 2006;75:435–65. https://doi.org/10.1146/annurev.biochem.74.082803.133500.
13. Singh CK, Chhabra G, Ndiaye MA, Garcia-Peterson LM, Mack NJ, Ahmad N. The role of sirtuins in antioxidant and redox signaling. Antioxid Redox Signal. 2018;28(8):643–61. https://doi.org/10.1089/ars.2017.7290.
14. Lu G, Li J, Zhang H, Zhao X, Yan LJ, Yang X. Role and possible mechanisms of Sirt1 in depression. Oxid Med Cell Longev. 2018;2018:8596903. https://doi.org/10.1155/2018/8596903.
15. Takada Y, Singh S, Aggarwal BB. Identification of a p65 peptide that selectively inhibits NF-kappa B activation induced by various inflammatory stimuli and its role in down-regulation of NF-kappaB-mediated gene expression and up-regulation of apoptosis. J Biol Chem. 2004;279(15):15096–104. https://doi.org/10.1074/jbc.M311192200.

16. Gu L, Tao X, Xu Y, Han X, Qi Y, Xu L, et al. Dioscin alleviates BDL- and DMN-induced hepatic fibrosis via Sirt1/Nrf2-mediated inhibition of p38 MAPK pathway. Toxicol Appl Pharmacol. 2016;292:19–29. https://doi.org/10.1016/j.taap.2015.12.024.
17. Robledinos-Anton N, Fernandez-Gines R, Manda G, Cuadrado A. Activators and inhibitors of NRF2: A review of their potential for clinical development. Oxid Med Cell Longev. 2019;2019:9372182. https://doi.org/10.1155/2019/9372182.
18. Bouvier E, Brouillard F, Molet J, Claverie D, Cabungcal JH, Cresto N, et al. Nrf2-dependent persistent oxidative stress results in stress-induced vulnerability to depression. Mol Psychiatry. 2017;22(12):1701–13. https://doi.org/10.1038/mp.2016.144.
19. Zhu X, Guo F, Tang H, Huang C, Xie G, Huang T, et al. Islet transplantation attenuating testicular injury in type 1 diabetic rats Is associated with suppression of oxidative stress and inflammation via Nrf-2/HO-1 and NF-kappaB pathways. J Diabetes Res. 2019;2019:8712492. https://doi.org/10.1155/2019/8712492.
20. Dixon SJ, Lemberg KM, Lamprecht MR, Skouta R, Zaitsev EM, Gleason CE, et al. Ferroptosis: an iron-dependent form of nonapoptotic cell death. Cell. 2012;149(5):1060–72. https://doi.org/10.1016/j.cell.2012.03.042.
21. Stockwell BR, Friedmann Angeli JP, Bayir H, Bush AI, Conrad M, Dixon SJ, et al. Ferroptosis: A regulated cell death nexus linking metabolism, redox biology, and disease. Cell. 2017;171(2):273–85. https://doi.org/10.1016/j.cell.2017.09.021.
22. Deng HF, Yue LX, Wang NN, Zhou YQ, Zhou W, Liu X, et al. Mitochondrial iron overload-mediated inhibition of Nrf2-HO-1/GPX4 assisted ALI-induced nephrotoxicity. Front Pharmacol. 2020;11:624529. https://doi.org/10.3389/fphar.2020.624529.
23. Song X, Long D. Nrf2 and Ferroptosis: A new research direction for neurodegenerative diseases. Front Neurosci. 2020;14:267. https://doi.org/10.3389/fnins.2020.00267.
24. Friedmann Angeli JP, Schneider M, Proneth B, Tyurina YY, Tyurin VA, Hammond VJ, et al. Inactivation of the ferroptosis regulator Gpx4 triggers acute renal failure in mice. Nat Cell Biol. 2014;16(12):1180–91. https://doi.org/10.1038/ncb3064.
25. Brigelius-Flohe R, Flohe L. Regulatory phenomena in the glutathione peroxidase superfamily. Antioxid Redox Signal. 2020;33(7):498–516. https://doi.org/10.1089/ars.2019.7905.
26. Hattori H, Imai H, Kirai N, Furuhama K, Sato O, Konishi K, et al. Identification of a responsible promoter region and a key transcription factor, CCAAT/enhancer-binding protein epsilon, for up-regulation of PHGPx in HL60 cells stimulated with TNF alpha. Biochem J. 2007;408(2):277–86. https://doi.org/10.1042/BJ20070245.
27. Hattori H, Imai H, Furuhama K, Sato O, Nakagawa Y. Induction of phospholipid hydroperoxide glutathione peroxidase in human polymorphonuclear neutrophils and HL60 cells stimulated with TNF-alpha. Biochem Biophys Res Commun. 2005;337(2):464–73. https://doi.org/10.1016/j.bbrc.2005.09.076.

28. Sriram CS, Jangra A, Gurjar SS, Mohan P, Bezbaruah BK. Edaravone abrogates LPS-induced behavioral anomalies, neuroinflammation and PARP-1. Physiol Behav. 2016;154:135–44. https://doi.org/10.1016/j.physbeh.2015.10.029.
29. Rothstein JD. Edaravone: A new drug approved for ALS. Cell. 2017;171(4):725. https://doi.org/10.1016/j.cell.2017.10.011.
30. Pan Y, Li W, Feng Y, Xu J, Cao H. Edaravone attenuates experimental asthma in mice through induction of HO-1 and the Keap1/Nrf2 pathway. Exp Ther Med. 2020;19(2):1407–16. https://doi.org/10.3892/etm.2019.8351.
31. Liu J, Jiang Y, Zhang G, Lin Z, Du S. Protective effect of edaravone on blood-brain barrier by affecting NRF-2/HO-1 signaling pathway. Exp Ther Med. 2019;18(4):2437–42. https://doi.org/10.3892/etm.2019.7859.
32. Herbet M, Natorska-Chomicka D, Ostrowska M, Gawronska-Grzywacz M, Izdebska M, Piatkowska-Chmiel I, et al. Edaravone presents antidepressant-like activity in corticosterone model of depression in mice with possible role of Fkbp5, Comt, Adora1 and Slc6a15 genes. Toxicol Appl Pharmacol. 2019;380:114689. https://doi.org/10.1016/j.taap.2019.114689.
33. Jangra A, Sriram CS, Dwivedi S, Gurjar SS, Hussain MI, Borah P, et al. Sodium phenylbutyrate and Edaravone abrogate chronic restraint stress-induced behavioral deficits: implication of oxido-nitrosative, endoplasmic reticulum stress cascade, and neuroinflammation. Cell Mol Neurobiol. 2017;37(1):65–81. https://doi.org/10.1007/s10571-016-0344-5.
34. Golden SA, Covington HE, 3rd, Berton O, Russo SJ. A standardized protocol for repeated social defeat stress in mice. Nat Protoc. 2011;6(8):1183–91. https://doi.org/10.1038/nprot.2011.361.
35. Prut L, Belzung C. The open field as a paradigm to measure the effects of drugs on anxiety-like behaviors: a review. Eur J Pharmacol. 2003;463(1–3):3–33. https://doi.org/10.1016/s0014-2999(03)01272-x.
36. Tye KM, Prakash R, Kim SY, Fenno LE, Grosenick L, Zarabi H, et al. Amygdala circuitry mediating reversible and bidirectional control of anxiety. Nature. 2011;471(7338):358–62. https://doi.org/10.1038/nature09820.
37. Sawangjit A, Oyanedel CN, Niethard N, Salazar C, Born J, Inostroza M. The hippocampus is crucial for forming non-hippocampal long-term memory during sleep. Nature. 2018;564(7734):109–13. https://doi.org/10.1038/s41586-018-0716-8.
38. Wang W, Wang T, Bai S, Chen Z, Qi X, Xie P. Dl-3-n-butylphthalide attenuates mouse behavioral deficits to chronic social defeat stress by regulating energy metabolism via AKT/CREB signaling pathway. Transl Psychiatry. 2020;10(1):49. https://doi.org/10.1038/s41398-020-0731-z.
39. Koolhaas JM, Korte SM, De Boer SF, Van Der Vegt BJ, Van Reenen CG, Hopster H, et al. Coping styles in animals: current status in behavior and stress-physiology. Neurosci Biobehav Rev. 1999;23(7):925–35. https://doi.org/10.1016/s0149-7634(99)00026-3.
40. Cui Y, Hu S, Hu H. Lateral Habenular Burst Firing as a Target of the Rapid Antidepressant Effects of Ketamine. Trends Neurosci. 2019;42(3):179–91. https://doi.org/10.1016/j.tins.2018.12.002.

41. Cerniauskas I, Winterer J, de Jong JW, Lukacsovich D, Yang H, Khan F, et al. Chronic Stress Induces Activity, Synaptic, and Transcriptional Remodeling of the Lateral Habenula Associated with Deficits in Motivated Behaviors. Neuron. 2019;104(5):899–915 e8. https://doi.org/10.1016/j.neuron.2019.09.005.
42. Jiao SS, Yao XQ, Liu YH, Wang QH, Zeng F, Lu JJ, et al. Edaravone alleviates Alzheimer's disease-type pathologies and cognitive deficits. Proc Natl Acad Sci U S A. 2015;112(16):5225–30. https://doi.org/10.1073/pnas.1422998112.
43. Manji HK, Drevets WC, Charney DS. The cellular neurobiology of depression. Nat Med. 2001;7(5):541–7. https://doi.org/10.1038/87865.
44. Fenn AM, Gensel JC, Huang Y, Popovich PG, Lifshitz J, Godbout JP. Immune activation promotes depression 1 month after diffuse brain injury: a role for primed microglia. Biol Psychiatry. 2014;76(7):575–84. https://doi.org/10.1016/j.biopsych.2013.10.014.
45. Skaper SD, Facci L, Giusti P. Neuroinflammation, microglia and mast cells in the pathophysiology of neurocognitive disorders: a review. CNS Neurol Disord Drug Targets. 2014;13(10):1654–66. https://doi.org/10.2174/1871527313666141130224206.
46. Grozio A, Sociali G, Sturla L, Caffa I, Soncini D, Salis A, et al. CD73 protein as a source of extracellular precursors for sustained NAD+ biosynthesis in FK866-treated tumor cells. J Biol Chem. 2013;288(36):25938–49. https://doi.org/10.1074/jbc.M113.470435.
47. Libert S, Pointer K, Bell EL, Das A, Cohen DE, Asara JM, et al. SIRT1 activates MAO-A in the brain to mediate anxiety and exploratory drive. Cell. 2011;147(7):1459–72. https://doi.org/10.1016/j.cell.2011.10.054.
48. consortium C. Sparse whole-genome sequencing identifies two loci for major depressive disorder. Nature. 2015;523(7562):588–91. https://doi.org/10.1038/nature14659.
49. Feng S, Yang Q, Liu M, Li W, Yuan W, Zhang S, et al. Edaravone for acute ischaemic stroke. Cochrane Database Syst Rev. 2011;(12):CD007230. https://doi.org/10.1002/14651858.CD007230.pub2.
50. Belleau EL, Treadway MT, Pizzagalli DA. The impact of stress and major depressive disorder on hippocampal and medial prefrontal cortex morphology. Biol Psychiatry. 2019;85(6):443–53. https://doi.org/10.1016/j.biopsych.2018.09.031.
51. Treadway MT, Waskom ML, Dillon DG, Holmes AJ, Park MTM, Chakravarty MM, et al. Illness progression, recent stress, and morphometry of hippocampal subfields and medial prefrontal cortex in major depression. Biol Psychiatry. 2015;77(3):285–94. https://doi.org/10.1016/j.biopsych.2014.06.018.
52. Allen J, Romay-Tallon R, Brymer KJ, Caruncho HJ, Kalynchuk LE. Mitochondria and mood: mitochondrial dysfunction as a key player in the manifestation of depression. Front Neurosci. 2018;12:386. https://doi.org/10.3389/fnins.2018.00386.
53. Gardner A, Boles RG. Beyond the serotonin hypothesis: mitochondria, inflammation and neurodegeneration in major depression and affective spectrum disorders. Prog

Neuropsychopharmacol Biol Psychiatry. 2011;35(3):730–43. https://doi.org/10.1016/j.pnpbp.2010.07.030.

54. Alcocer-Gomez E, de Miguel M, Casas-Barquero N, Nunez-Vasco J, Sanchez-Alcazar JA, Fernandez-Rodriguez A, et al. NLRP3 inflammasome is activated in mononuclear blood cells from patients with major depressive disorder. Brain Behav Immun. 2014;36:111–7. https://doi.org/10.1016/j.bbi.2013.10.017.
55. Zha L, Yu Z, Fang J, Zhou L, Guo W, Zhou J. NLRC3 delays the progression of AD in APP/PS1 mice via inhibiting PI3K activation. Oxid Med Cell Longev. 2020;2020:5328031. https://doi.org/10.1155/2020/5328031.
56. Bansal Y, Kuhad A. Mitochondrial dysfunction in depression. Curr Neuropharmacol. 2016;14(6):610–8. https://doi.org/10.2174/1570159x14666160229114755.
57. Klinedinst NJ, Regenold WT. A mitochondrial bioenergetic basis of depression. J Bioenerg Biomembr. 2015;47(1–2):155–71. https://doi.org/10.1007/s10863-014-9584-6.
58. Liu L, Zhou X, Zhang Y, Pu J, Yang L, Yuan S, et al. Hippocampal metabolic differences implicate distinctions between physical and psychological stress in four rat models of depression. Transl Psychiatry. 2018;8(1):4. https://doi.org/10.1038/s41398-017-0018-1.
59. Kishi T, Yoshimura R, Kitajima T, Okochi T, Okumura T, Tsunoka T, et al. SIRT1 gene is associated with major depressive disorder in the Japanese population. J Affect Disord. 2010;126(1–2):167–73. https://doi.org/10.1016/j.jad.2010.04.003.
60. Abe-Higuchi N, Uchida S, Yamagata H, Higuchi F, Hobara T, Hara K, et al. Hippocampal Sirtuin 1 signaling mediates depression-like behavior. Biol Psychiatry. 2016;80(11):815–26. https://doi.org/10.1016/j.biopsych.2016.01.009.
61. Liao D, Lv C, Cao L, Yao D, Wu Y, Long M, et al. Curcumin attenuates chronic unpredictable mild stress-induced depressive-like behaviors via restoring changes in oxidative stress and the activation of Nrf2 signaling pathway in rats. Oxid Med Cell Longev. 2020;2020:9268083. https://doi.org/10.1155/2020/9268083.
62. Martin-de-Saavedra MD, Budni J, Cunha MP, Gomez-Rangel V, Lorrio S, Del Barrio L, et al. Nrf2 participates in depressive disorders through an anti-inflammatory mechanism. Psychoneuroendocrinology. 2013;38(10):2010–22. https://doi.org/10.1016/j.psyneuen.2013.03.020.
63. Mendez-David I, Tritschler L, Ali ZE, Damiens MH, Pallardy M, David DJ, et al. Nrf2-signaling and BDNF: A new target for the antidepressant-like activity of chronic fluoxetine treatment in a mouse model of anxiety/depression. Neurosci Lett. 2015;597:121–6. https://doi.org/10.1016/j.neulet.2015.04.036.
64. Bian H, Wang G, Huang J, Liang L, Zheng Y, Wei Y, et al. Dihydrolipoic acid protects against lipopolysaccharide-induced behavioral deficits and neuroinflammation via regulation of Nrf2/HO-1/NLRP3 signaling in rat. J Neuroinflammation. 2020;17(1):166. https://doi.org/10.1186/s12974-020-01836-y.

65. Dodson M, Castro-Portuguez R, Zhang DD. NRF2 plays a critical role in mitigating lipid peroxidation and ferroptosis. Redox Biol. 2019;23:101107. https://doi.org/10.1016/j.redox.2019.101107.
66. Olagnier D, Brandtoft AM, Gunderstofte C, Villadsen NL, Krapp C, Thielke AL, et al. Nrf2 negatively regulates STING indicating a link between antiviral sensing and metabolic reprogramming. Nat Commun. 2018;9(1):3506. https://doi.org/10.1038/s41467-018-05861-7.
67. Jia M, Qin D, Zhao C, Chai L, Yu Z, Wang W, et al. Redox homeostasis maintained by GPX4 facilitates STING activation. Nat Immunol. 2020;21(7):727–35. https://doi.org/10.1038/s41590-020-0699-0.
68. Adzic M, Brkic Z, Mitic M, Francija E, Jovicic MJ, Radulovic J, et al. Therapeutic strategies for treatment of inflammation-related depression. Curr Neuropharmacol. 2018;16(2):176–209. https://doi.org/10.2174/1570159X15666170828163048.
69. Ren JX, Sun X, Yan XL, Guo ZN, Yang Y. Ferroptosis in neurological diseases. Front Cell Neurosci. 2020;14:218. https://doi.org/10.3389/fncel.2020.00218.

Figures

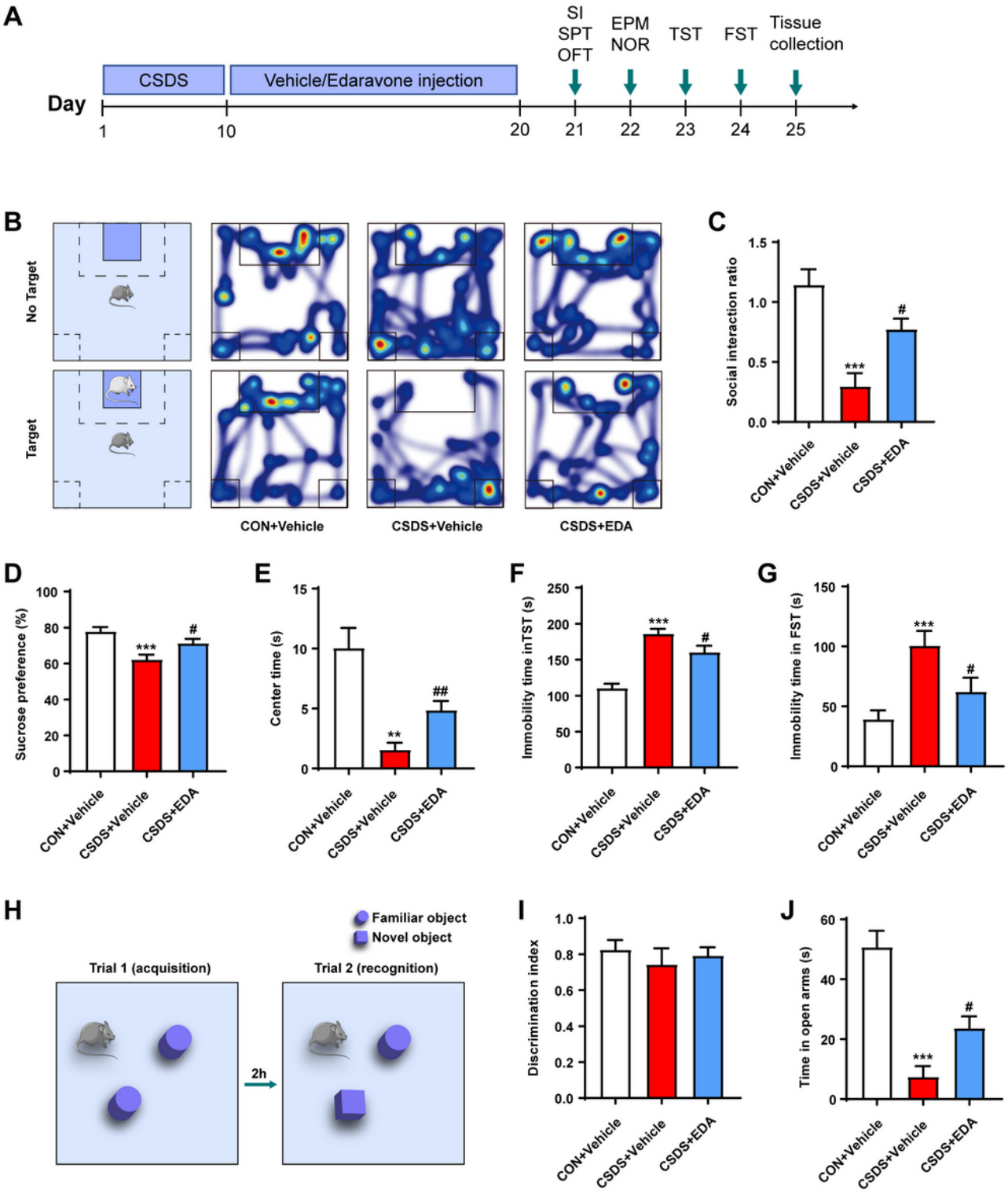

Figure 1

Effects of EDA on CSDS-induced depressive and anxiety like behaviors. a A schematic representation of the CSDS procedure and treatments in mice. b Heat maps of path tracing in the social interaction test after EDA administration. c Social interaction test. d Sucrose preference test. e Open field test. f Tail suspension test. g Forced swimming test. h-i Novel object recognition test. j Elevated plus maze test. All

the data are expressed as mean ± SEM (n = 10 per group). **p < 0.01, ***p < 0.001 versus the CON + Vehicle group. #p < 0.05, ##p < 0.01 versus the CSDS + Vehicle group.

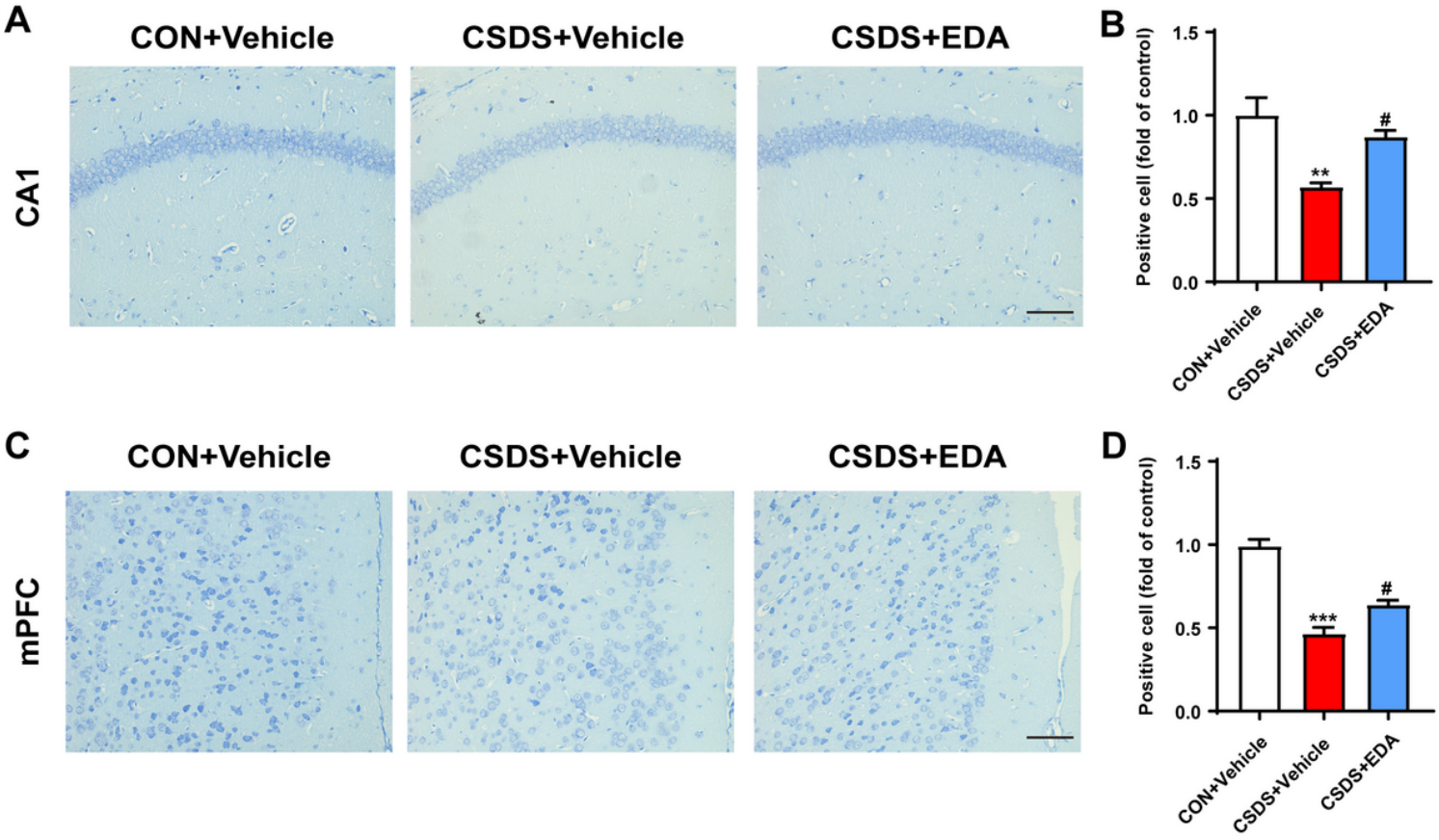

Figure 2

Influence of EDA on neuronal death in the Hip and mPFC. a-b Nissl staining in the hippocampal CA1 subregion and its statistical analysis c-d Nissl staining in the mPFC and its statistical analysis. Data are presented as mean ± SEM (n = 3 per group). Scale bars, 50 μm. **p < 0.01, ***p < 0.001 versus the CON + Vehicle group. #p < 0.05 versus the CSDS + Vehicle group.

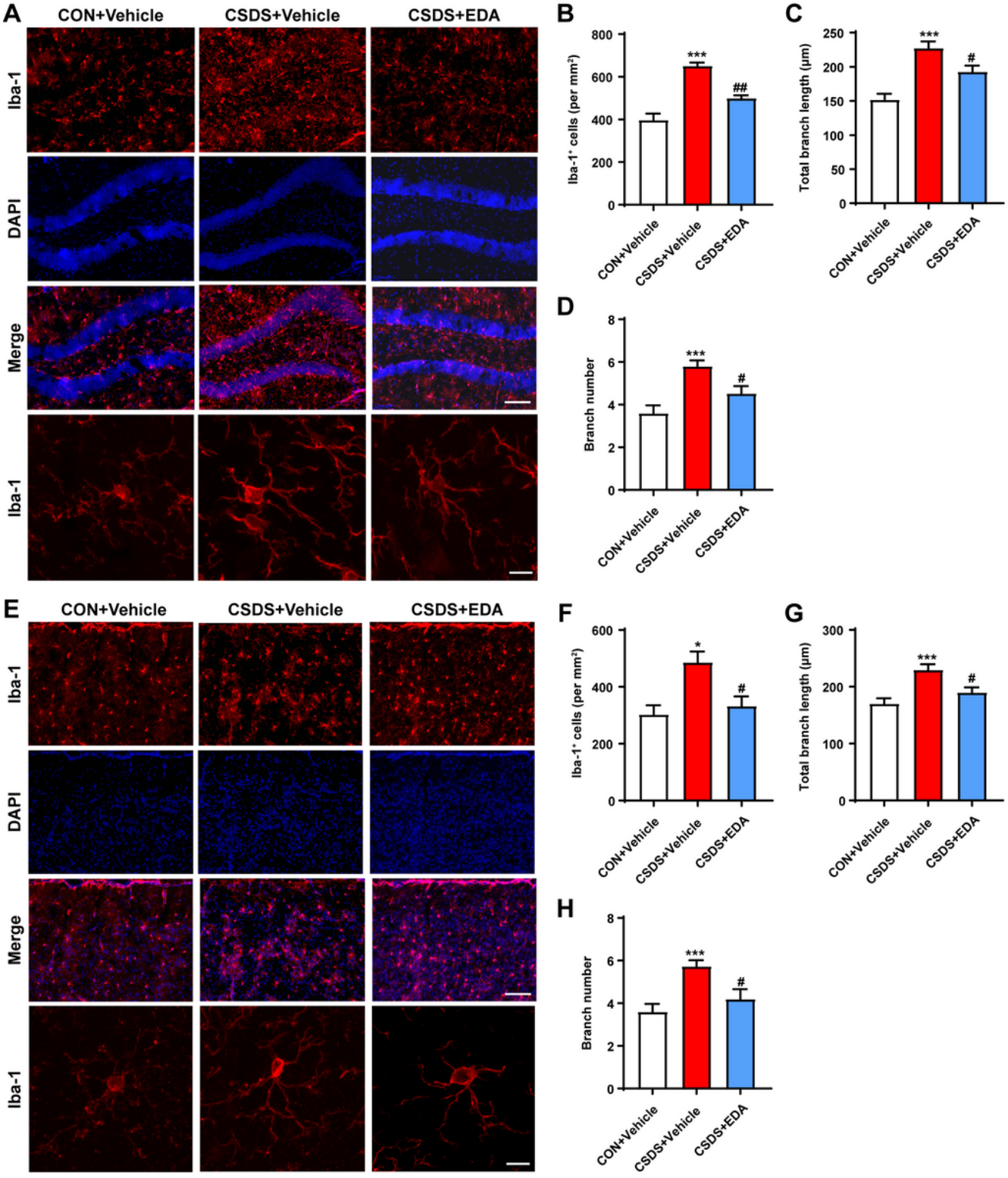

Figure 3

Effects of EDA on microglial activation in the CSDS mouse Hip and mPFC. a EDA inhibited microglial activation in the CSDS mouse Hip. Representative images of microglia immunostaining for Iba-1. Scale bars, 100 μm (upper panel) and 10 μm (lower panel). b Quantification of Iba-1 positive cells per mm2 in the mouse Hip. c Total branch length. d Branch number. e EDA inhibited microglial activation in the CSDS mouse mPFC. Representative images of microglia immunostaining for Iba-1. Scale bars, 100 μm (upper

panel) and 10 μm (lower panel). f Quantification of Iba-1 positive cells per mm2 in the mouse Hip. g Total branch length. h Branch number. All the data are presented as mean ± SEM (n = 3 mice/group,15 cells/group). *p < 0.05, ***p < 0.001 versus the CON + Vehicle group. #p < 0.05, ##p < 0.01 versus the CSDS + Vehicle group.

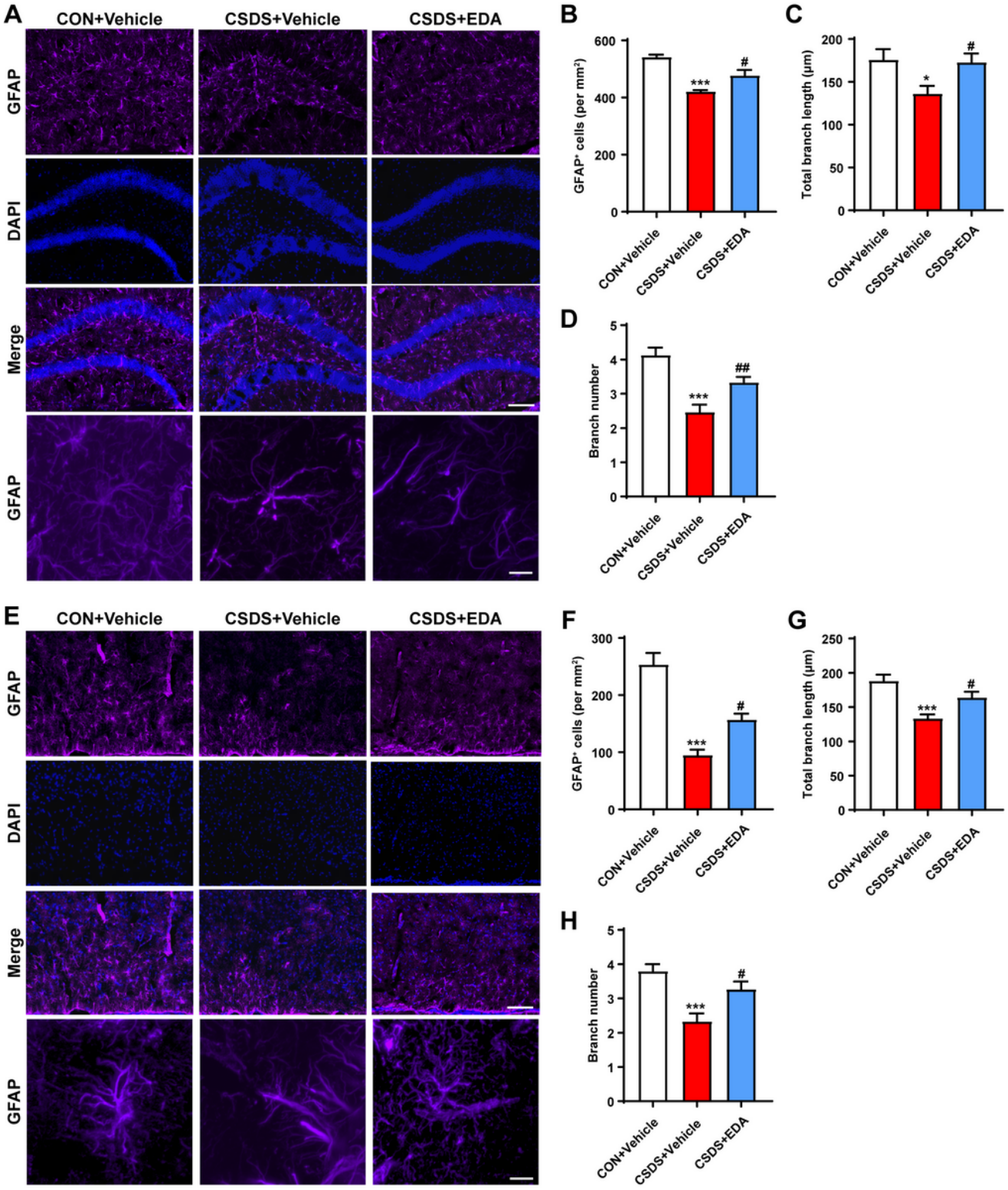

Figure 4

Effects of EDA on astrocyte loss in the CSDS mouse Hip and mPFC. a Effect of EDA on astrocyte dysfunction induced by CUS in the Hip. Representative images of astrocyte immunostaining for GFAP. Scale bars, 100 μm (upper panel) and 10 μm (lower panel). b Quantification of GFAP-positive cells per mm2 in the mouse Hip. c Total branch length. d Branch number. e Effect of EDA on astrocyte loss induced by CUS in the mPFC. Representative images of astrocyte immunostaining for GFAP. Scale bars, 100 μm (upper panel) and 10 μm (lower panel). f Quantification of GFAP-positive cells per mm2 in the mouse Hip. g Total branch length. h Branch number. All the data are presented as mean ± SEM (n = 3 mice/group,15 cells/group). *p < 0.05, ***p < 0.001 versus the CON + Vehicle group. #p < 0.05, ##p < 0.01 versus the CSDS + Vehicle group.

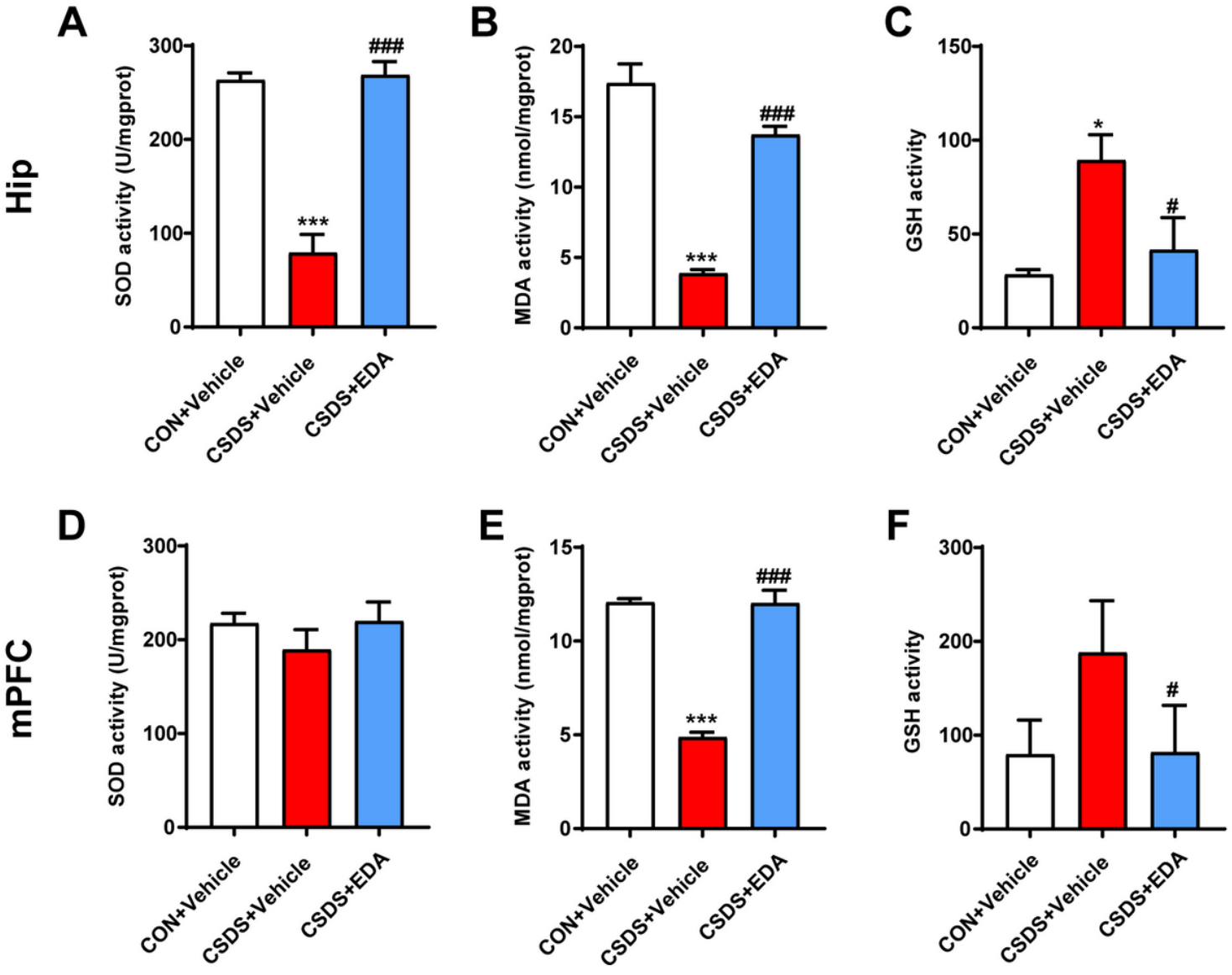

Figure 5

The changes of oxidative stress parameters in the Hip and mPFC after EDA exposure. a-c The levels of oxidative stress parameters including MDA, SOD and GSH in the Hip. d-f MDA content, the activities of

SOD and GSH in the mPFC. Data are presented as mean ± SEM (n = 6 per group). *p < 0.05, ***p < 0.001 versus the CON + Vehicle group. #p < 0.05, ###p < 0.001 versus the CSDS + Vehicle group.

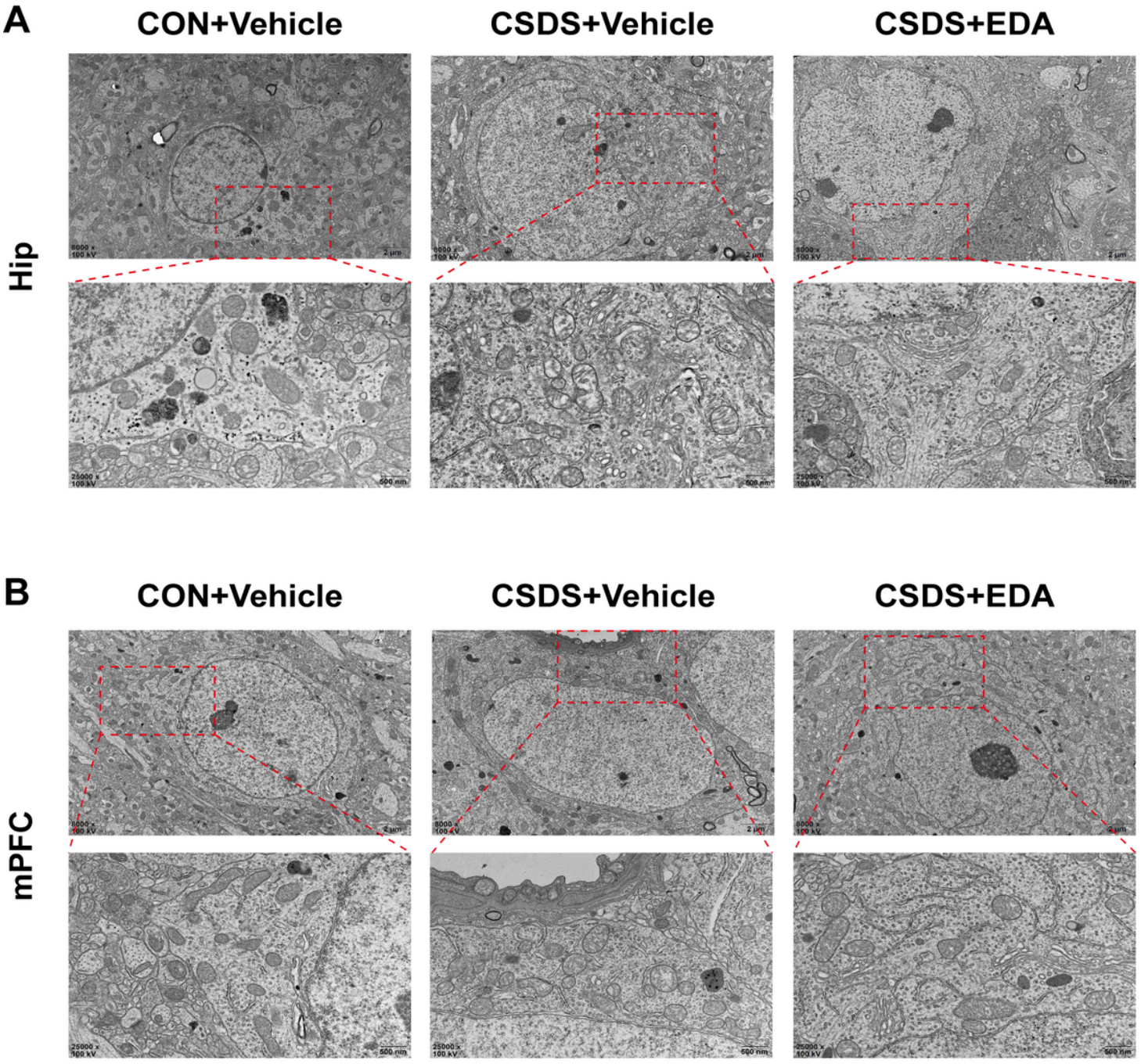

Figure 6

Ultrastructure of neurons in the CSDS model of Hip and mPFC with EDA treatment. a Electron micrographs showed mitochondrial damages and in the hippocampal neuron (red arrows) Scale bars, 2 μm (upper panel) and 500 nm (lower panel). b Electron micrographs showed mitochondrial damages and in the mPFC neuron (red arrows). Scale bars, 2 μm (upper panel) and 500 nm (lower panel).

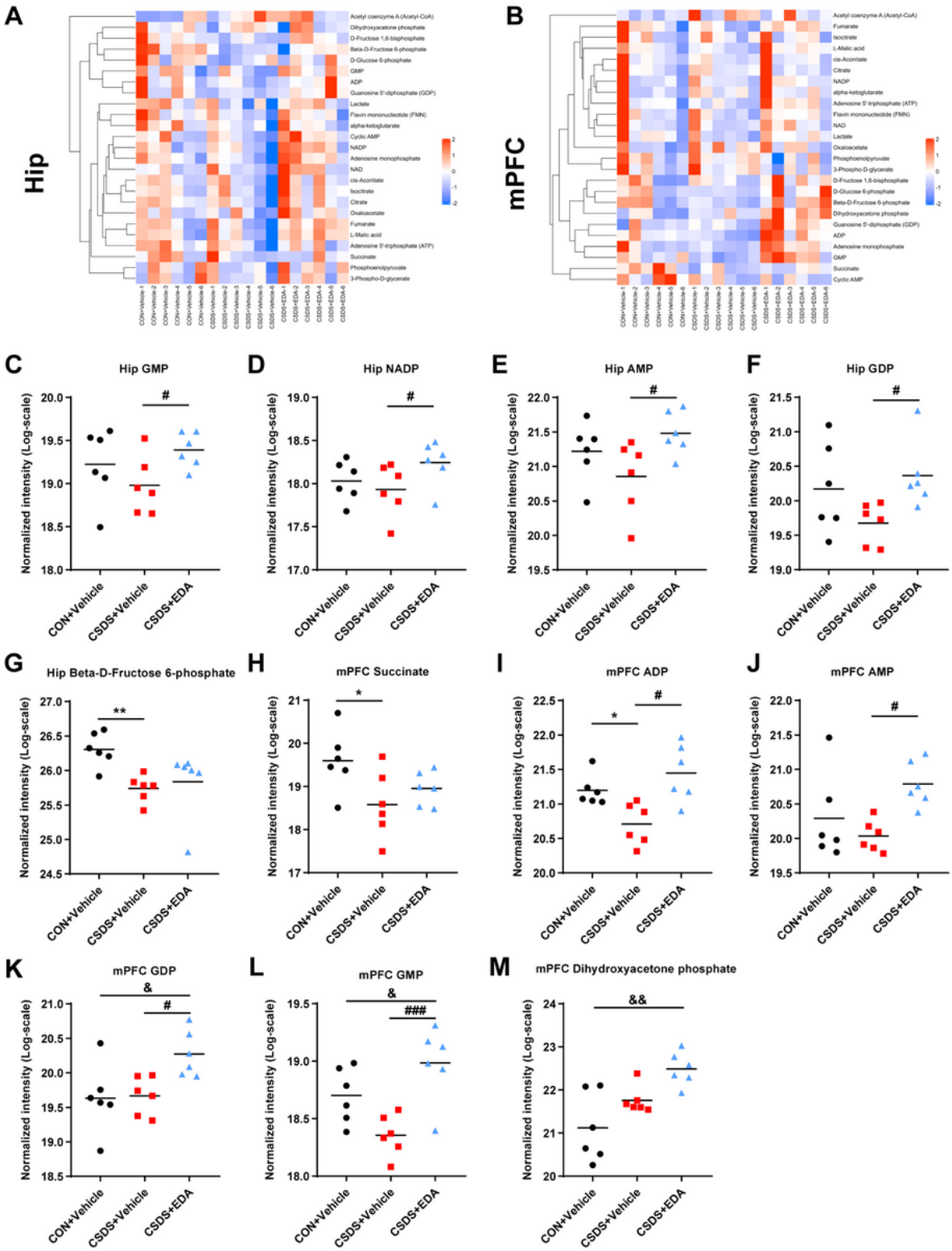

Figure 7

Targeted energy metabolomics in the Hip and mPFC of CSDS model mice. a Heatmap of partly energy-related metabolites in the Hip b Heatmap of partly energy-related metabolites in the mPFC. Rows indicate metabolites. The degree of change in metabolite concentration is color coded. c-g Differential energy metabolites in the Hip. h-m Differential energy metabolites in the mPFC . GMP : guanosine 5'-monophosphate; NADP : nicotinamide-adenine-dinucleotide phosphate; ADP : adenosine-5'-diphosphate; GDP:

guanosine 5'-diphosphate. AMP: adenosine monophosphate. Data are presented as mean ± SEM (n = 6 per group). *p < 0.05, **p < 0.01 versus the CON + Vehicle group. #p < 0.05, ###p < 0.001 versus the CSDS + Vehicle group. &p < 0.05, &&p < 0.01 versus the CSDS + EDA group.

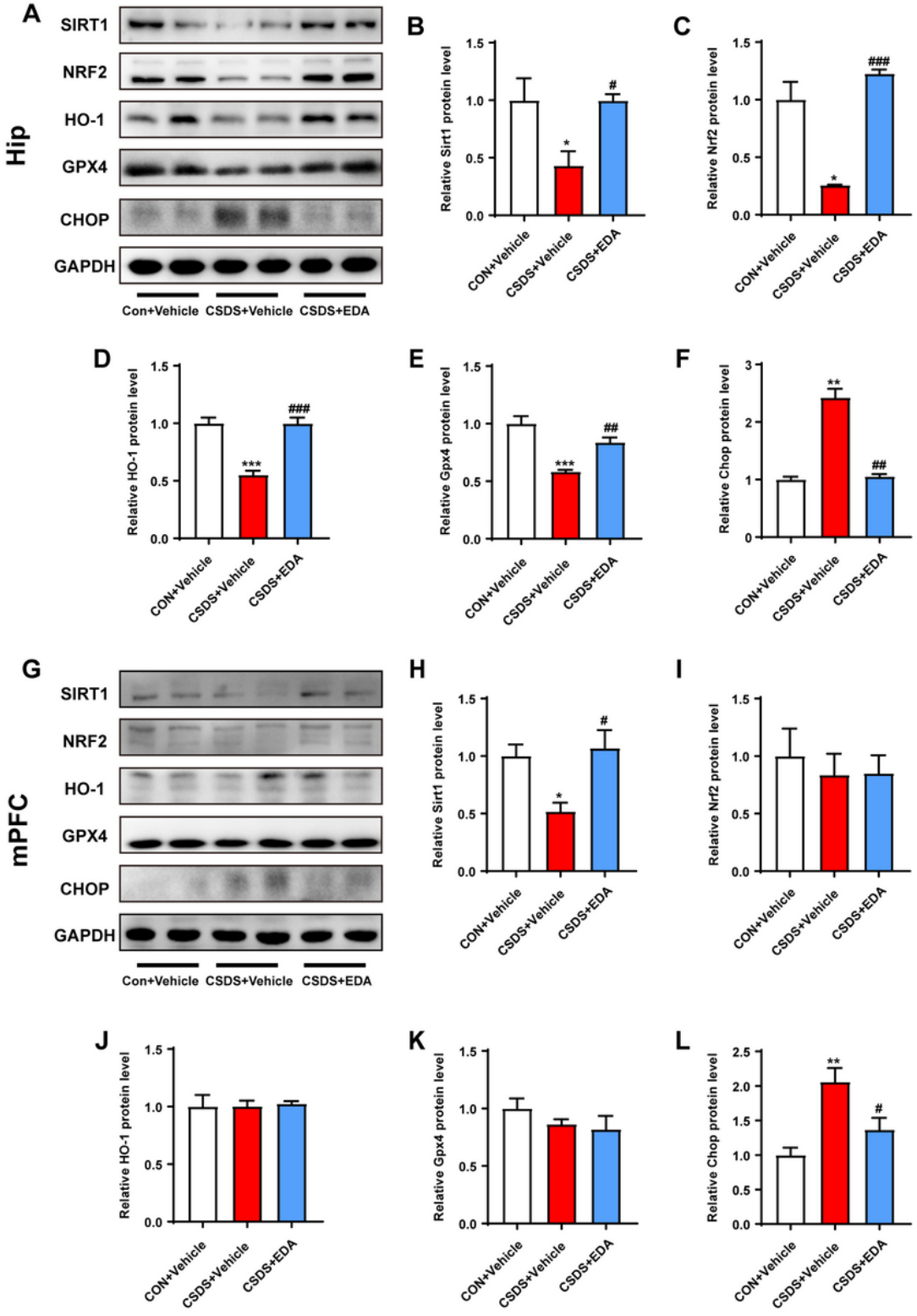

Figure 8

Effect of EDA on Sirt1/Nrf2/HO-1/Gpx4 signaling pathway and endoplasmic reticulum stress. a Representative WB bands in the hippocampal region. b-f statistical graphs of relative protein expression

of Sirt1 (b), Nrf2 (c), HO-1 (d),Gpx4 (e), and Chop (f). g Representative WB bands in the mPFC region. h-l Statistical graphs of relative protein expression of Sirt1 (h), Nrf2 (i), HO-1 (j), Gpx4 (k), and Chop (l). Data are presented as mean ± SEM (n = 4 per group). *p < 0.05, **p < 0.01, ***p < 0.001 versus the CON + Vehicle group. #p < 0.05, ##p < 0.01, ###p < 0.001 versus the CSDS + Vehicle group.

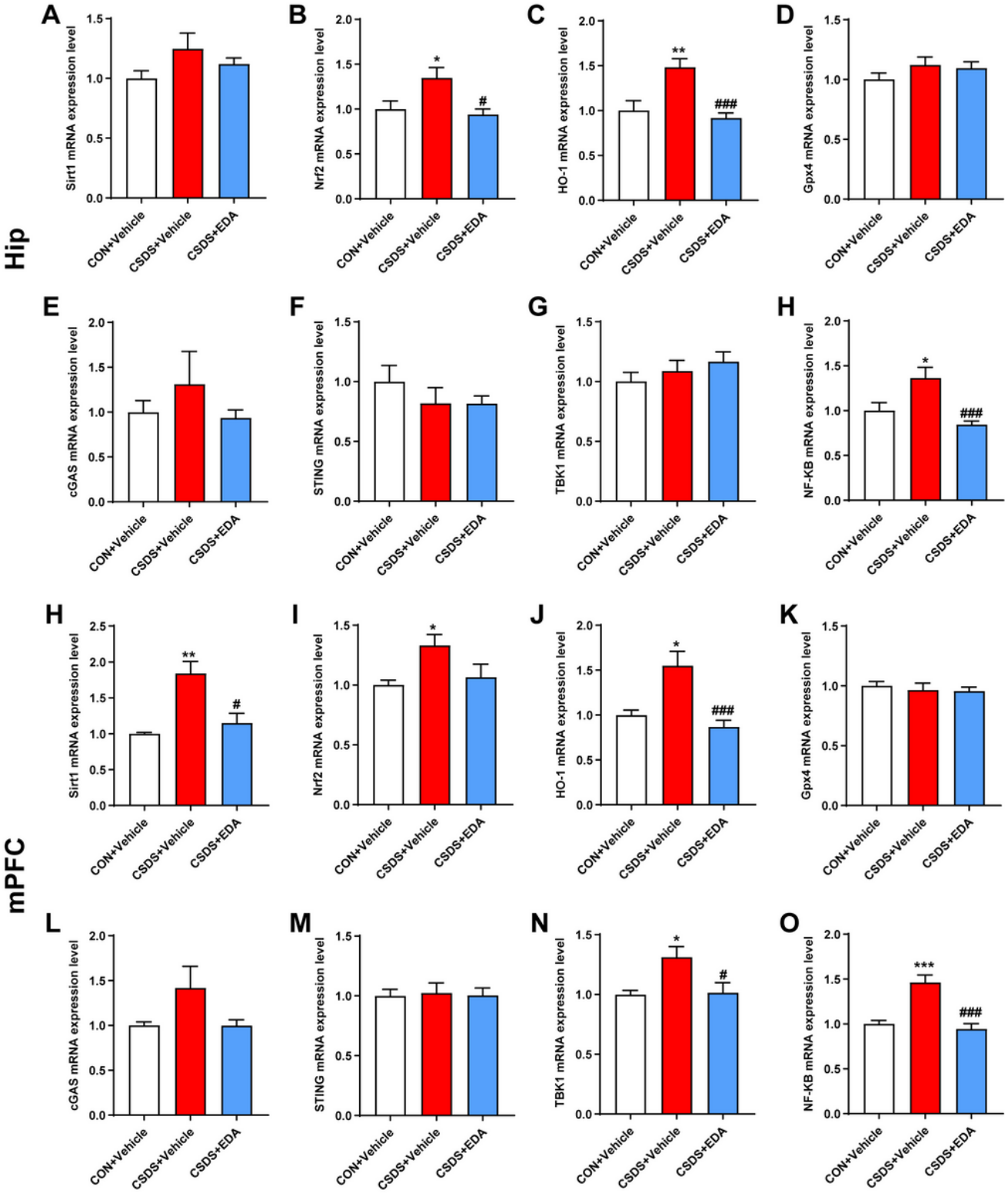

Figure 9

Effect of EDA on Sirt1/Nrf2/HO-1/Gpx4 pathway in mRNA expression levels. a-h The mRNA expression of Sirt1 (a), Nrf2 (b), HO-1 (c), Gpx4 (d), cGAS (e), STING (f), TBK1 (g), and NF-κB (h) in the hippocampal region. h-o The mRNA expression of Sirt1 (h), Nrf2 (i), HO-1 (j), Gpx4 (k), cGAS (l), STING (m), TBK1 (n), and NF-κB (o) in the mPFC region. Data are presented as mean ± SEM (n = 8 per group). *p < 0.05, **p < 0.01, ***p < 0.001 versus the CON + Vehicle group. #p < 0.05, ###p < 0.001 versus the CSDS + Vehicle group.

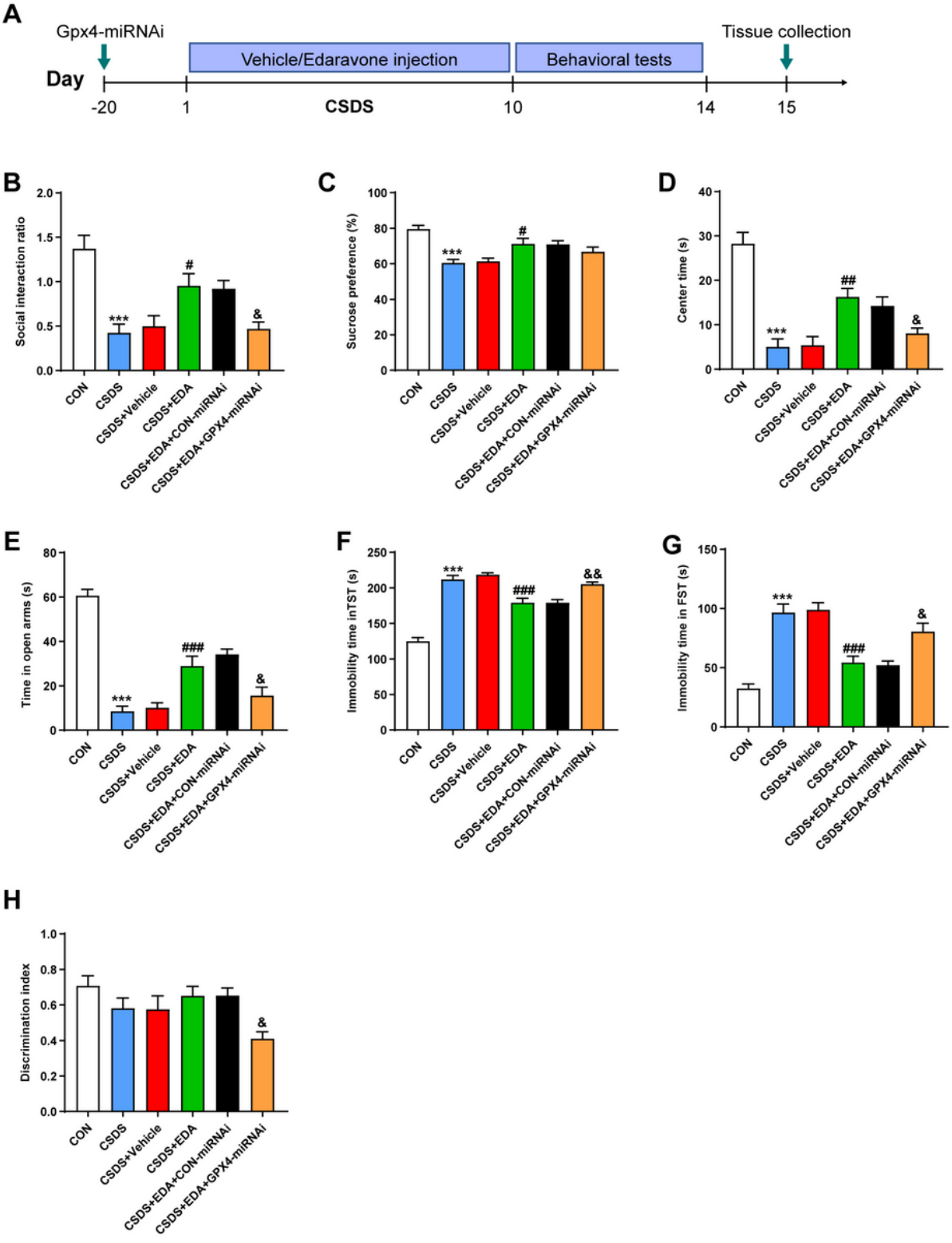

Figure 10

Knockdown Gpx4 in the Hip antagonized the antidepressant and anxiolytic effects of EDA. a Schematic timeline of the experimental procedure. b Social interaction test. c Sucrose preference test. d Open field test. e Tail suspension test. f Forced swimming test. g Novel object recognition test. h Elevated plus maze test. All the data are expressed as mean ± SEM (n = 10 per group). ***p < 0.001 versus the CON group. #p < 0.05, ##p < 0.01, ###p < 0.001 versus the CSDS group. &p < 0.05, &&p < 0.01 versus the CSDS + EDA group.

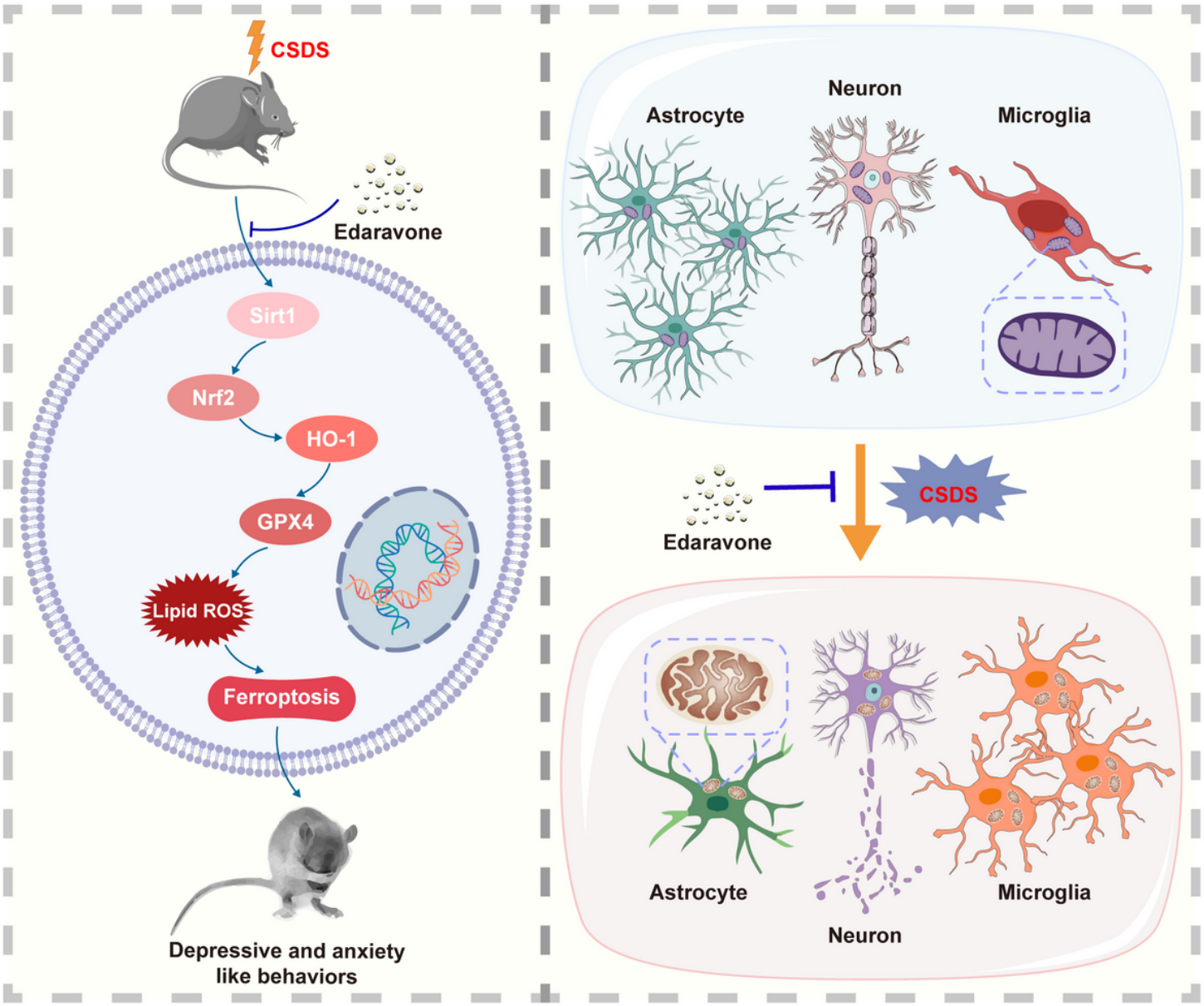

Figure 11

A schematic illustration of the proposed mechanisms underlying EDA-related antidepressant and anxiolytic efficacy.

Supplementary Files

This is a list of supplementary files associated with this preprint. Click to download.

- Fig.S1.tif
- Fig.S2.tif
- SupplementaryMaterial.doc